LEVEL II

(14) SDAC-TR-77-5

(12)

(6) STUDY OF SELECTED EVENTS IN THE BAIKAL RIFT ZONE IN A SEISMIC DISCRIMINATION CONTEXT

(9) Technical rept.,

(10) P.A. SOBEL, D.H. VON SEGGERN, E.I. SWEETSER & D.W. RIVERS

Seismic Data Analysis Center

Teledyne Geotech, 314 Montgomery Street, Alexandria, Virginia 22314

(11) 17 OCTOBER 1977 (12) 71 p.

Sponsored by

The Defense Advanced Research Projects Agency (DARPA)

(15) F08606-78-C-0007 ARPA Order No. 2551

Monitored By

AFTAC/VSC

312 Montgomery Street, Alexandria, Virginia 22314

408 258

Thelma Spring

Unclassified

SECURITY CLASSIFICATION OF THIS PAGE (When Data Entered)

REPORT DOCUMENTATION PAGE		READ INSTRUCTIONS BEFORE COMPLETING FORM
1. REPORT NUMBER SDAC-TR-77-5	2. GOVT ACCESSION NO.	3. RECIPIENT'S CATALOG NUMBER
4. TITLE (and Subtitle) STUDY OF SELECTED EVENTS IN THE BAIKAL RIFT ZONE IN A SEISMIC DISCRIMINATION CONTEXT		5. TYPE OF REPORT & PERIOD COVERED Technical 6. PERFORMING ORG. REPORT NUMBER
7. AUTHOR(s) P. A. Sobel, E. I. Sweetser, D. H. von Seggern, D. W. Rivers		8. CONTRACT OR GRANT NUMBER(s) F08606-78-C-0007
9. PERFORMING ORGANIZATION NAME AND ADDRESS Teledyne Geotech 314 Montgomery Street Alexandria, Virginia 22314		10. PROGRAM ELEMENT, PROJECT, TASK AREA & WORK UNIT NUMBERS VT/8709
11. CONTROLLING OFFICE NAME AND ADDRESS Defense Advanced Research Projects Agency Nuclear Monitoring Research Office 1400 Wilson Blvd. Arlington, Virginia 22209		12. REPORT DATE 17 October 1977 13. NUMBER OF PAGES 70
14. MONITORING AGENCY NAME & ADDRESS(if different from Controlling Office) VELA Seismological Center 312 Montgomery Street Alexandria, Virginia 22314		15. SECURITY CLASS. (of this report) Unclassified 15a. DECLASSIFICATION/DOWNGRADING SCHEDULE

16. DISTRIBUTION STATEMENT (of this Report)

APPROVED FOR PUBLIC RELEASE; DISTRIBUTION UNLIMITED.

17. DISTRIBUTION STATEMENT (of the abstract entered in Block 20, if different from Report)

18. SUPPLEMENTARY NOTES

Author's Report Date 06/13/77

19. KEY WORDS (Continue on reverse side if necessary and identify by block number)

Baikal Rift Zone
Underground Nuclear Explosions
Seismic Discrimination
M_s versus m_b

20. ABSTRACT (Continue on reverse side if necessary and identify by block number)

Six events from the Baikal rift zone occurring from 1971 to 1975 were examined in a seismic discrimination context. Seismograms from ALPA, LASA, NORSAR, the HGLP, the WWSSN, and the SRO stations were studied for source mechanism, M_S-m_b, corner frequency, pP, complexity, and spectral ratio. All the Baikal events can be identified as earthquakes except the November 5, 1976, event which shows explosion characteristics. The characteristics of the Baikal events were compared to six East Kazakh explosions and the Aleutian explosion MILROW. No evidence is found, from the signals studied here, for a zone of high attenuation under the

CONT'

DD FORM 1 JAN 73 1473 EDITION OF 1 NOV 65 IS OBSOLETE

Unclassified

SECURITY CLASSIFICATION OF THIS PAGE (When Data Entered)

Baikal rift. The discriminants found to be useful in this study, with the possible exception of short-period spectral ratio which is rather unreliable, would not give correct discrimination for a suitable shot array. However there is a full magnitude range of separation in $M_s:m_b$ in this region, suggesting that a suitable shot array might be difficult to devise.

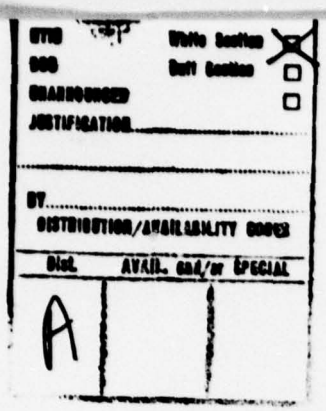

LEVEL II

(12)

STUDY OF SELECTED EVENTS IN THE BAIKAL RIFT ZONE IN A SEISMIC DISCRIMINATION CONTEXT

SEISMIC DATA ANALYSIS CENTER REPORT NO.: SDAC-TR-77-5

AFTAC Project Authorization No.:	VELA T/8709/B/PMP
Project Title:	Seismic Data Analysis Center
ARPA Order No.:	2551
ARPA Program Code No.:	7F10
Name of Contractor:	TELEDYNE GEOTECH
Contract No.:	F08606-78-C-0007
Date of Contract:	01 October 1977
Amount of Contract:	$2,674,245
Contract Expiration Date:	30 September 1978
Project Manager:	Robert R. Blandford (703) 836-3882

P. O. Box 334, Alexandria, Virginia 22314

APPROVED FOR PUBLIC RELEASE; DISTRIBUTION UNLIMITED.

ABSTRACT

Six events from the Baikal rift zone occurring from 1971 to 1975 were examined in a seismic discrimination context. Seismograms from ALPA, LASA, NORSAR, the HGLP, the WWSSN, and the SRO stations were studied for source mechanism, M_s-m_b, corner frequency, pP, complexity, and spectral ratio. All the Baikal events can be identified as earthquakes except the November 5, 1976, event which shows explosion characteristics. The characteristics of the Baikal events were compared to six East Kazakh explosions and the Aleutian explosion MILROW. No evidence is found, from the signals studied here, for a zone of high attenuation under the Baikal rift. The discriminants found to be useful in this study, with the possible exception of short-period spectral ratio which is rather unreliable, would not give correct discrimination for a suitable shot array. However there is a full magnitude range of separation in M_s:m_b in this region, suggesting that a suitable shot array might be difficult to devise.

TABLE OF CONTENTS

LIST OF FIGURES

LIST OF FIGURES (Continued)

LIST OF TABLES

INTRODUCTION

Discrimination parameters have been applied in detail at only a few nuclear test sites and earthquake regions and the wide variability of path-related factors affecting discrimination is not yet fully revealed. This study is part of a series which will extend these discrimination studies to other regions of shallow earthquakes. This report examines six such events in the Baikal rift zone, which is shown in Figure 1. Most of the earthquakes in the Baikal rift zone are probably associated with normal faults bordering graben structures in the rift zone. Actual seismogram analysis revealed that the events chosen were too small to determine their exact fault plane solutions. We determine average M_s and m_b for the events in this study and apply other common discrimination parameters such as first motion, corner frequency, complexity, and short-period spectral ratios to the data. We examine source and propagation affects on the principle discrimination phases, P and LR. Results for the Baikal events will be compared to six East Kazakh explosions and the Aleutian explosion MILROW.

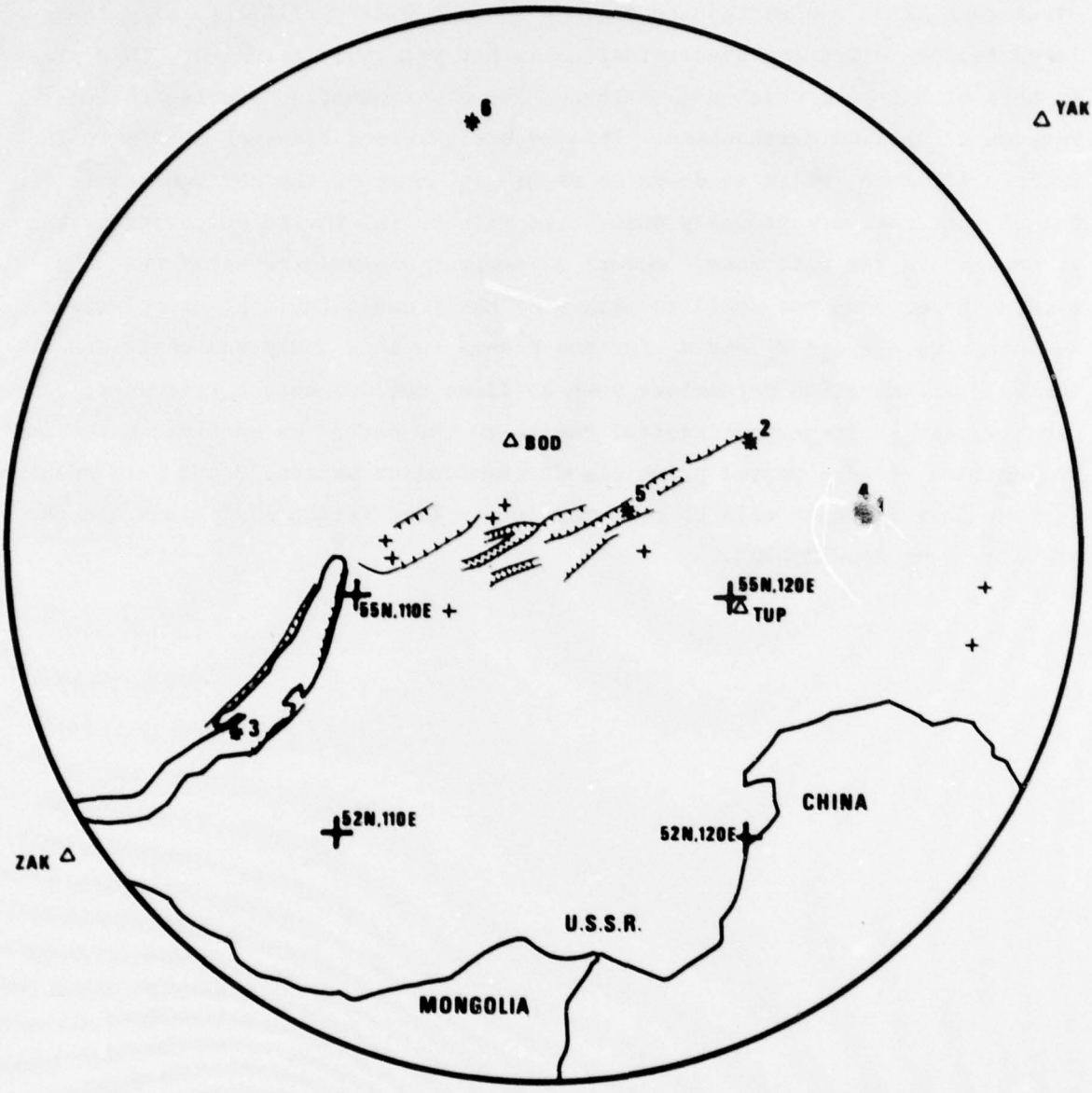

Figure 1. Map of the Baikal rift zone showing faults observed on satellite photographs and NEIS epicenters from January 1971 through February 1975.

TECTONIC SETTING

General Features

Figure 1 is a map of the Baikal rift zone, a system of grabens extending from Lake Baikal to about 2000 km northeast. The grabens are a geologically young feature situated in a Paleozoic fold belt. The Baikal rift zone is a region of normal faulting and crustal extension which may be a remote expression of the stress system resulting from the Indian-Eurasian collision (Molnar and Tapponnier, 1975). According to U.S.S.R. seismic studies (Solonenko, 1968), seismicity is confined to the crust.

Positive isostatic gravity anomalies follow the rift zone. The best explanation for these anomalies is a raised Moho boundary under the rift zone which overlies mantle of anomalously low density (Zorin, 1971). Heat flow measurements in Lake Baikal are higher than normal (Lubimova, 1969), confirming the magneto-telluric detection of a highly conducting layer in the upper mantle. Abnormal heating of the upper mantle beneath the rift zone may be causing the tectonic activity in this region.

Source Mechanisms of Earthquakes

Most of the earthquakes in the rift zone are associated with the normal faults which comprise the boundaries of the grabens (Solonenko, 1968; Molnar et al., 1973).

Molnar, P., and P. Tapponier (1975). Cenozoic tectonics of Asia: effects of a continental collision, Science, 189, 419.

Solonenko, V. P. (1968). Regional seismic zoning of the U.S.S.R. - Eastern Siberia, in Seismic Zoning of the U.S.S.R., edited by S. V. Medvedev, English translation, Keter Publishing House, Jerusalem.

Zorin, Y. (1971). Recent Structure and Isostasy of the Baikal Rift Zone and Surrounding Territory, Nauka, Moscow.

Lubimova, E. (1969). Heat flow patterns in Baikal and other rift zones, Tectonophysics, 8, 457.

Molnar, P., T. Fitch, and F. Wu (1973). Fault plane solutions of shallow earthquakes and contemporary tectonics in Asia, Earth and Planetary Science Letters, 19, 101.

NEIS epicenters for events in this area from January 1971 through February 1975 are shown in Figure 1 overlaying faults which were inferred from our satellite photomosaic of the area. Event 6 occurred in 1976 and was a special addition to the data set. It can be seen that the earthquakes are near the fault traces except for event 6. Studies of earthquake focal mechanisms in the Baikal region have shown that the tensile stresses are horizontally oriented, perpendicular to the trend of the grabens (Vvedenskaya, 1961).

Velocity, Density, and Attenuation

Seismic studies in the Baikal region report an average crustal thickness of 36 to 38 km in the rift zone and 36 to 46 km in the surrounding region (Beliayevsky et al., 1968). Geophysical studies indicate that the upper mantle under the rift zone has low velocities, low density, and possibly high attenuation (Rodean, 1976). Areas of high attenuation have also been observed southwest of the rift zone (Vinnik and Godzikovskaya, 1972, 1973). Table I shows a typical velocity profile in the rift zone derived from deep seismic sounding studies (Puzyrev et al., 1973).

The Baikal region has been compared with the African rift zone and has many features similar to the Basin-Range Province in the western United States, also a Cenozoic extensional region. Of special interest in this study is the degree of attenuation for P waves under the Baikal source region. High attenuation has been linked to positive travel-time residuals in the western United

---

Vvedenskaya, A. (1961). Special features of the stressed state in foci of earthquakes in the Baikal region, Izvestia, Geophys. Ser., 432.

Beliayevsky, N., A. Borisov, I. Valvovsky, and Y. Schukin (1968). Transcontinental crustal sections of the U.S.S.R. and adjacent areas, Canadian Journal of Earth Sciences, 5, 1067.

Rodean, H. (1976). Seismic yield verification and a regional M_s vs. m_b anomaly, Lawrence Livermore Laboratory, UCID-17006, 16 pp.

Vinnik, L., and A. Godzikovskaya (1972). Sounding of the Earth's mantle by the method of seismically conjugate points, Izvestia, Earth Physics, No. 10, 656.

Vinnik, L., and A. Godzikovskaya (1973). Lateral variations of the absorption by the upper mantle beneath Asia, Izvestia, Earth Physics, No. 1, 1.

Puzyrev, N., M. Mandelbaum, S. Krylov. B. Mishenkin, G. Krupskaya, and G. Petrick (1973), Deep seismic investigations in the Baikal rift zone, Tectonophysics, 20, 85.

TABLE I

Velocity Structure in the Baikal Rift Zone

Thickness (km)	P Velocity (km/sec)	Density (gm/cm^3)
6	5.8	2.7
9	6.0	2.8
23	6.4	2.9
mantle	7.8	3.2

States (Der, 1976); and in consideration of the similarities between the Baikal rift zone and the western United States, we investigated residuals for seismic stations located in this rift. Only four which regularly report to the ISC (International Seismological Center) are relevant: ZAK, BOD, TUP and YAK. These locations are shown in Figure 1; note that they are not in the rift zone proper. The 1974 ISC bulletins were gleaned for travel-time data at these stations for large earthquakes. An effort was made to sample somewhat evenly the teleseismic distance range and the full range of back azimuths. The residuals (relative to Jeffreys-Bullen tables) are plotted in Figure 2. In general, the residuals tend to negative times, implying higher upper mantle or crustal velocities for media under the stations. Even subsets for each station along that range of azimuth which would enclose rays emerging up under the Baikal rift zone do not apparently show a positive residual, although the data is probably too sparse and the stations are not well enough situated to draw definite conclusions.

Der, Z. A. (1976). On the existence, magnitude and causes of broad regional variations in body-wave amplitudes, SDAC-TR-76-8, Teledyne Geotech, Alexandria, Virginia.

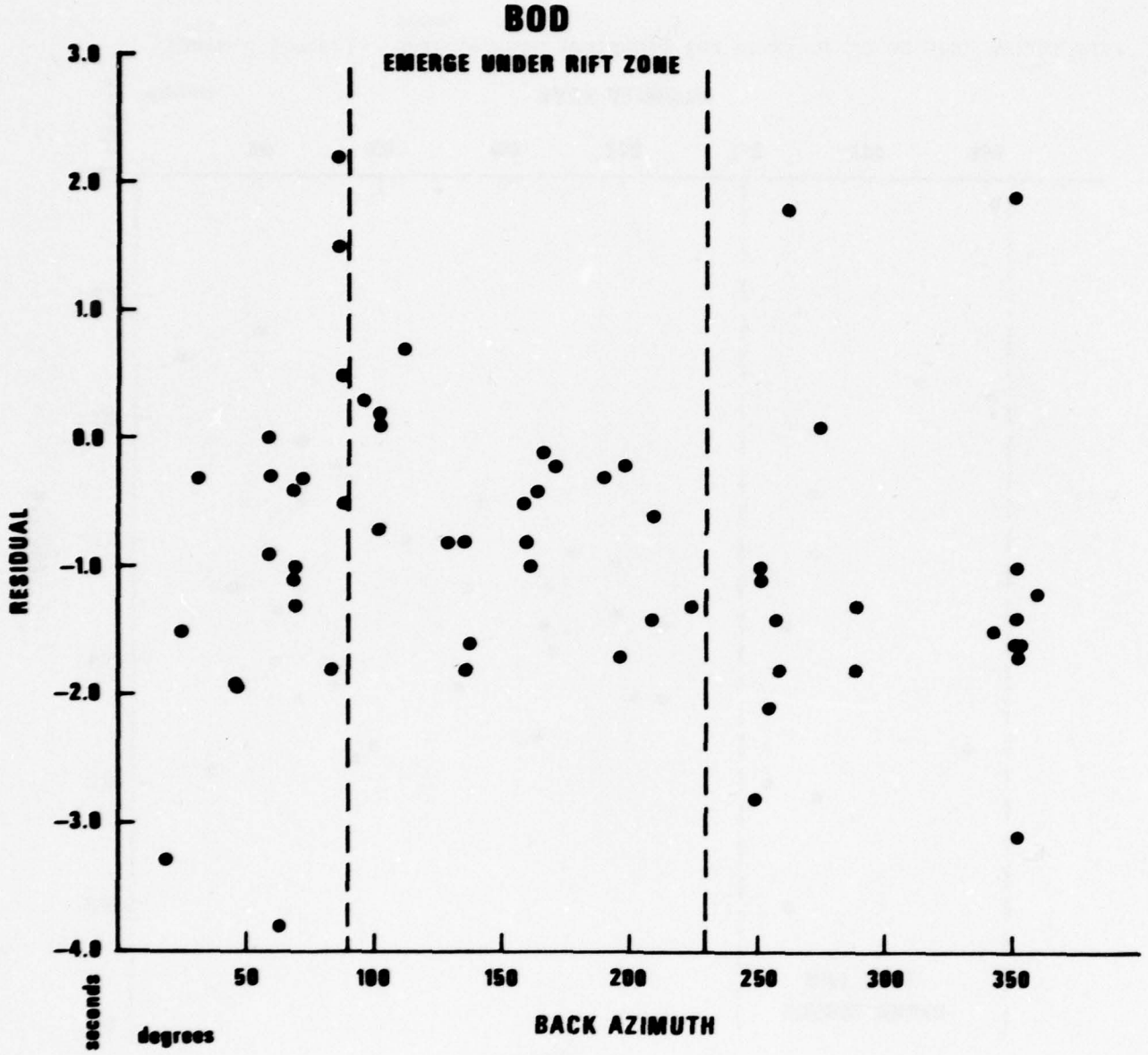

Figure 2. Selected ISC residuals for stations in or near Baikal rift zone.

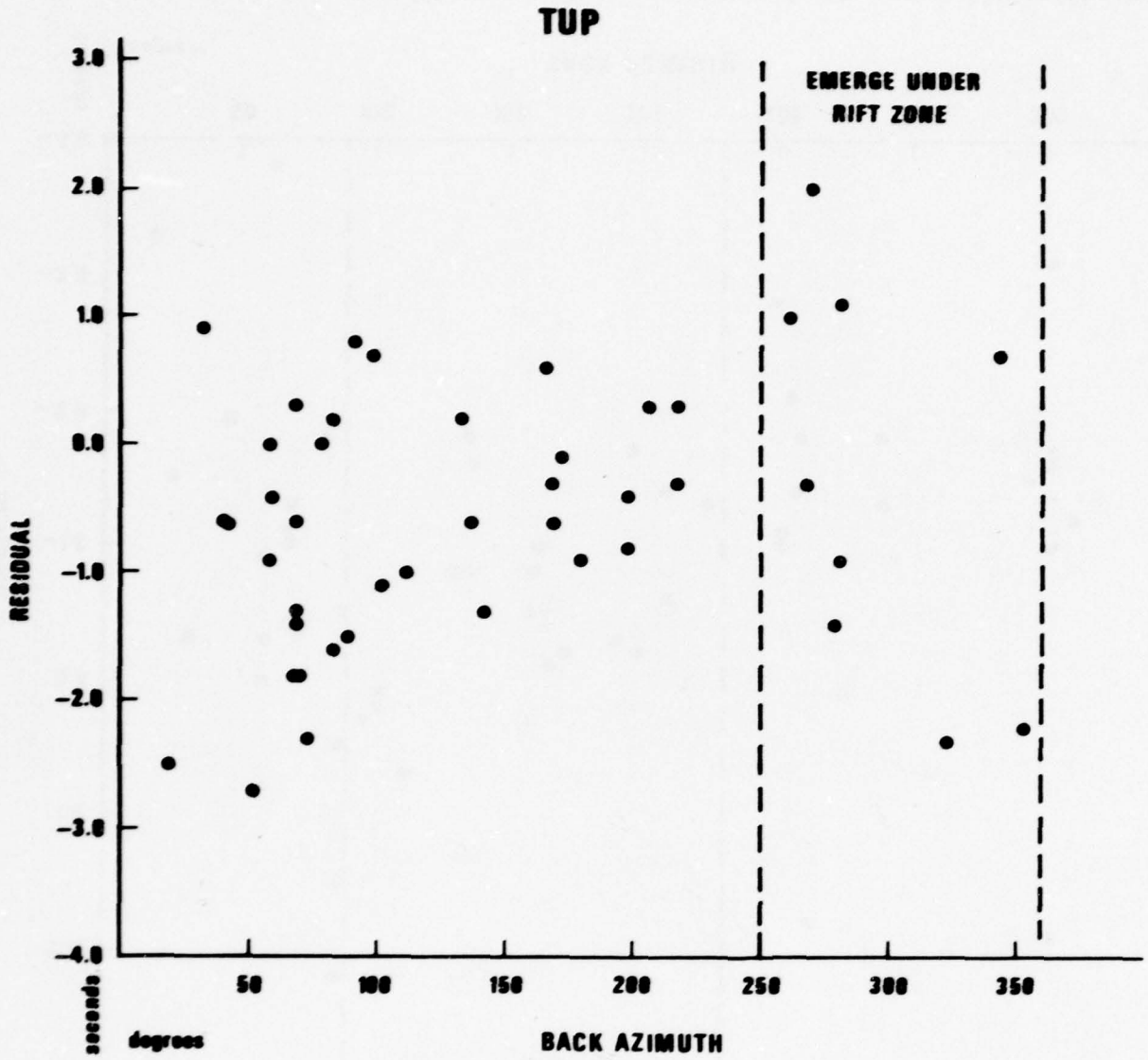

Figure 2 (cont.) Selected ISC residuals for stations in or near Baikal rift zone.

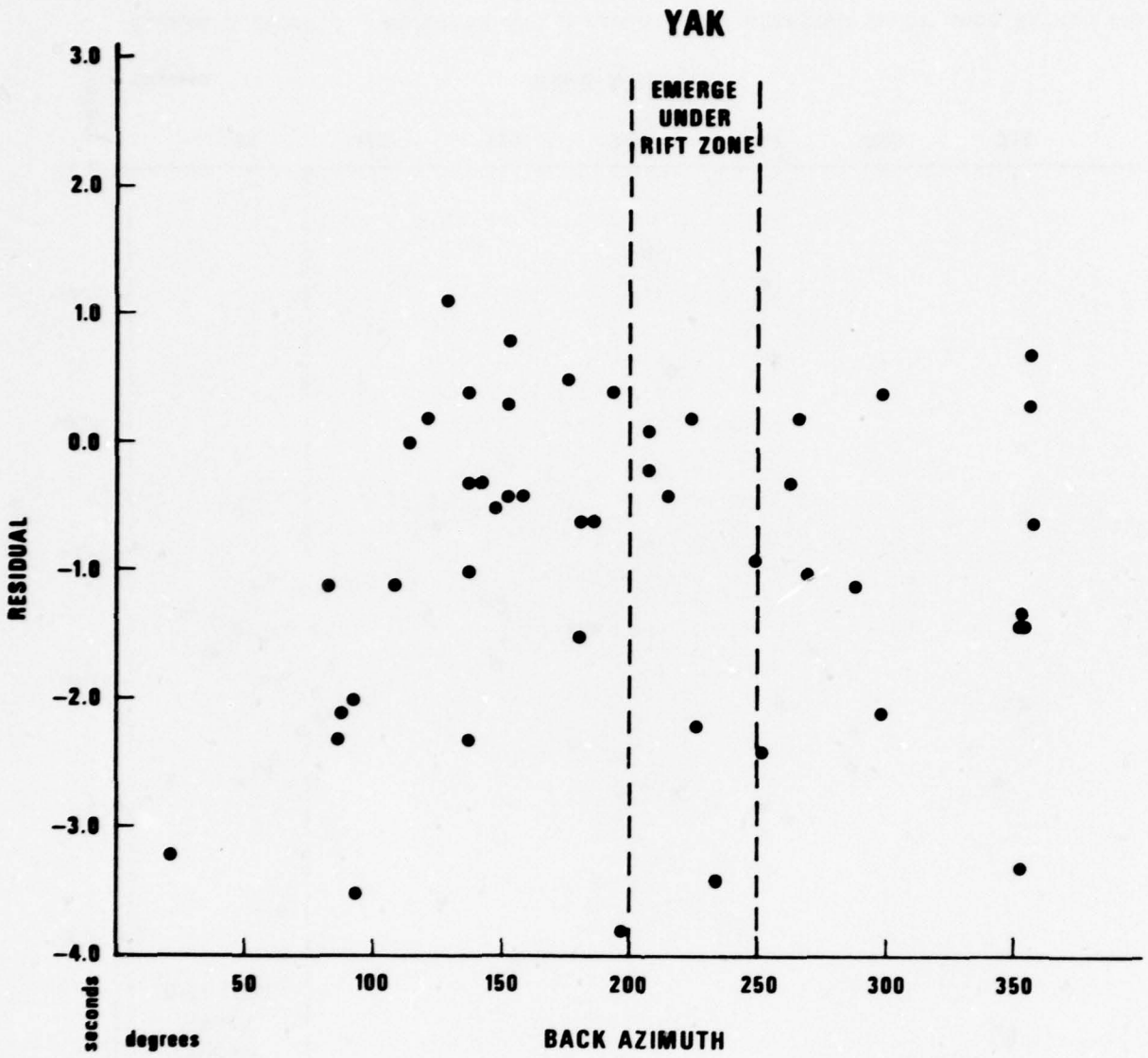

Figure 2 (cont.) Selected ISC residuals for stations in or near Baikal rift zone.

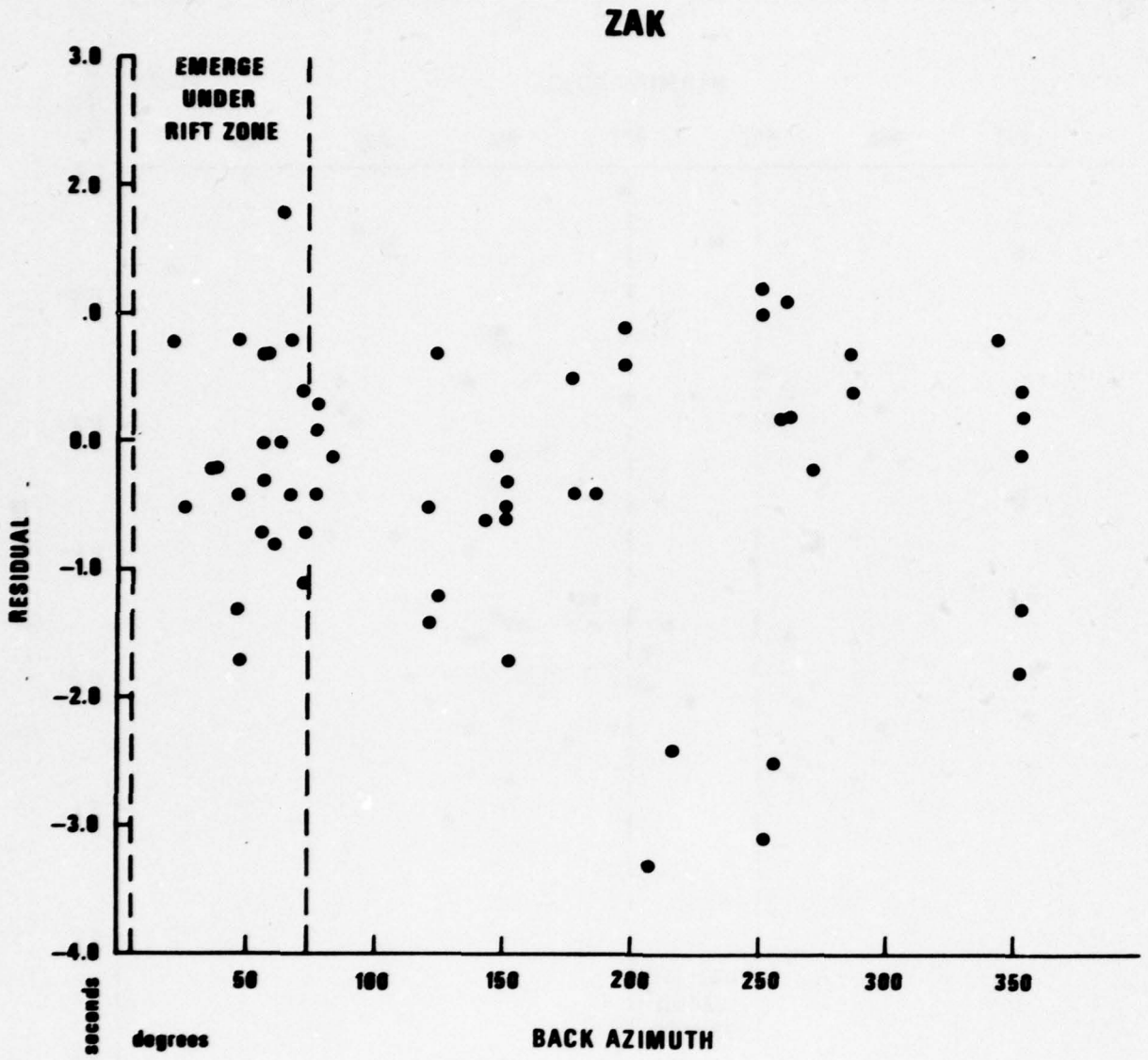

Figure 2 (cont.) Selected ISC residuals for stations in or near Baikal rift zone.

DATA

Earthquake Selection

For this study shallow-focus earthquakes were selected from the Baikal rift zone. The NEIS list locates the large majority of the earthquakes in the Baikal rift zone within the crust. The earthquakes chosen were limited to the years 1971 to 1975 so that we could utilize the data from the large seismic arrays and the HGLP network. We selected a total of six events as listed in Table II and shown in Figure 1. Again, we note that event 6 was in 1976 and added late to the data set. These particular six events were chosen on the basis of relatively low M_s, compared to m_b, as measured by Rayleigh waves recorded at NORSAR. Table II also lists the depths determined from our pP observations at LASA, NORSAR, and the average of selected WWSSN stations. All of the selected events are located within the crust.

Explosion Selection

The Baikal events were compared to explosions in East Kazakh, USSR, which lies to the southwest of the Baikal rift zone and to the Aleutian explosion MILROW. We selected a total of seven explosions as listed in Table III for this comparison.

Seismic Stations

Digital data from the three arrays ALPA, LASA, and NORSAR and from the available HGLP stations and film data from selected WWSSN stations were assembled for these events. The available LASA and NORSAR short-period P recordings are shown in Figure 3. We have used the AO subarray from LASA and the C3 subarray from NORSAR as in our previous reports of this series in order to avoid signal loss at high frequencies due to full-array beaming. WWSSN stations were selected on the basis of magnification and proximity to the region of study, and it is unlikely that stations not used here would significantly add to the data base for these Baikal events. Since WWSSN data was not available at the time of this study for event 6, we examined SRO data for this event instead of WWSSN data.

TABLE II

NEIS Parameters for Baikal Events

Event	Date	Origin Time	EPICENTER LAT (°N)	EPICENTER LONG (°E)	m_b	DEPTH NEIS	DEPTH LASA	DEPTH NORSAR	DEPTH This Study
1	14 Jun 1971	13 48 55.7	56.172	123.582	5.6	33	8	12	16
2	15 Jan 1972	18 07 57.8	57.426	120.664	4.7	13		12	16
3	9 Aug 1972	19 42 17.3	52.964	107.539	5.1	33	13		20
4	25 Nov 1972	13 42 34.4	56.290	123.464	5.1	33			23
5	21 Jun 1974	20 56 48.7	56.503	117.255	5.3	33	6	10	14
6*	05 Nov 1976	04 00 03.4	61.	113.	4.9			0	0

*Source parameters for event 6 are taken from the SDAC-NEP bulletin.

TABLE III

NEIS Parameters for East Kazakh and MILROW Explosions

Date	Origin Time	EPICENTER LAT (°N)	EPICENTER LONG (°E)	m_b	Region
2 Oct 1969	22 06 00.0	51.418	179.181	6.5	Aleutians
22 Mar 1971	04 32 57.8	49.744	78.185	5.8	East Kazakh
29 Nov 1971	06 02 57.1	49.758	78.126	5.5	East Kazakh
30 Dec 1971	06 20 57.7	49.750	78.130	5.8	East Kazakh
10 Feb 1972	05 02 57.3	49.986	78.886	5.5	East Kazakh
25 Jun 1974	03 56 57.6	49.889	78.115	4.8	East Kazakh
07 Dec 1974	05 59 56.9	49.908	77.648	4.8	East Kazakh

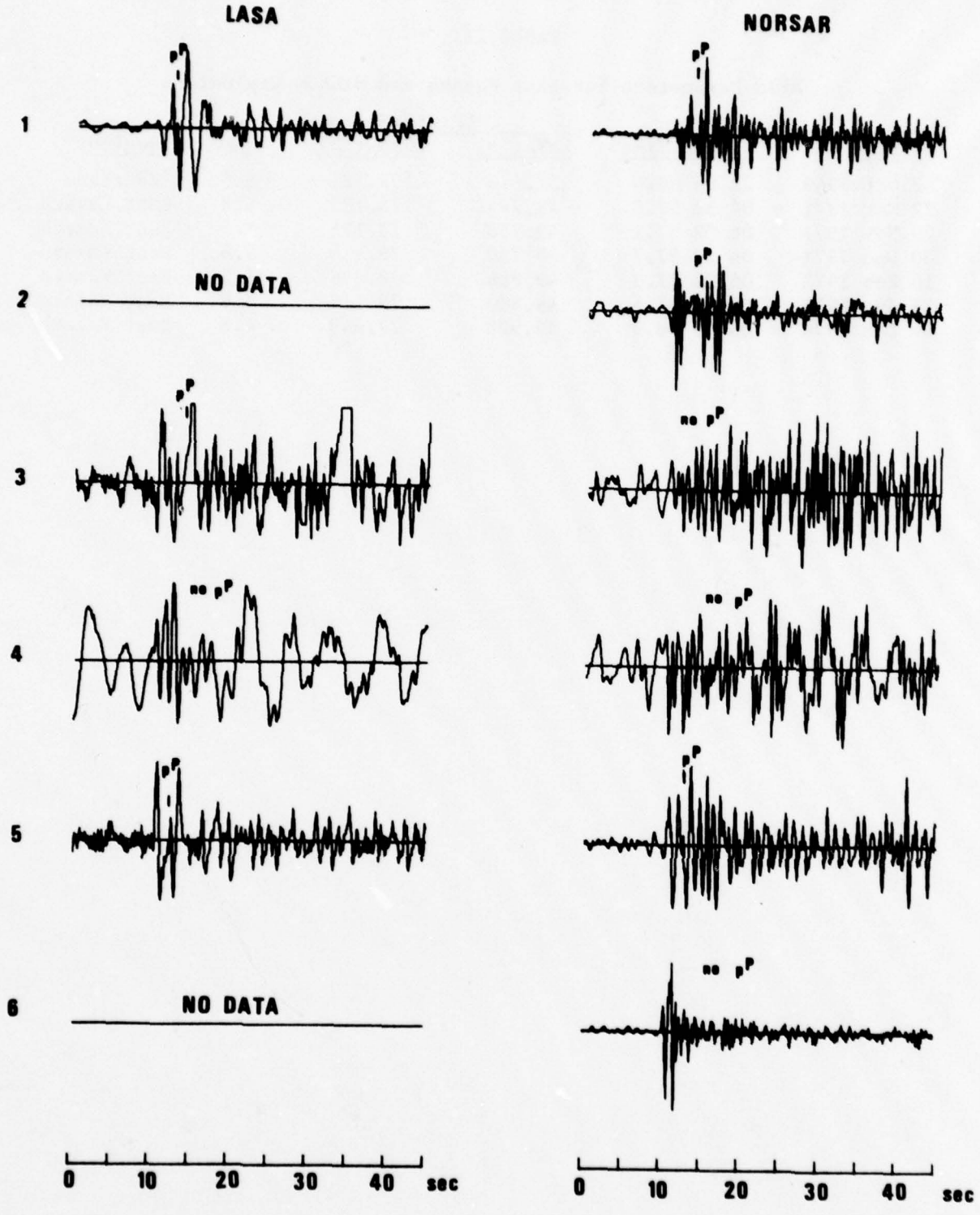

Figure 3. LASA and NORSAR short-period P recordings for the Baikal events studied.

SIGNAL ANALYSIS

Source Effects

We wanted initially to identify a source mechanism for each event so that we could predict the radiation pattern for body-wave and surface-wave phases. Determination of the fault planes for earthquakes whose magnitudes are below 6.0 is generally not reliable with teleseismic data, and all our earthquakes have m_b less than 6. First motions were determined when possible from the data we have collected, and ISC bulletin data was available for events 1 through 5. We have plotted all the first motions for the Baikal events in Figure 4. No clear first motions were available for event 6. Unfortunately, the short-period data were not consistent, and it is impossible on the basis of the plots alone to determine individual fault planes because dilatational and compressional first motions do not separate well. However, taken together, there is a dominance of dilatational first motion in the central part of the focal sphere plots; this would result from normal faulting and is in agreement with the body of known focal mechanisms for this region.

Corner frequencies and seismic moments for our Baikal events have been estimated from short-period LASA and NORSAR spectra. The spectra are shown in Figure 5. They are from the phased beams of the A0 subarray at LASA and C3 subarray at NORSAR. The sample length was 6.4 seconds. The signals have been tapered, and the instrument response was removed from the signal and noise spectra. Attenuation was removed from the spectra by multiplying by the factor $\exp(\pi f t^*)$ with a t^* of .59 for a ω^{-2} source model and .40 for a ω^{-3} source model at LASA and t^* of .18 for ω^{-2} and .00 (no attenuation) for ω^{-3} source models at NORSAR. The basis for these t^* values will be shown later in this report. Corner frequencies were estimated with the assumption of complete stress drop and a ω^{-2} or ω^{-3} asymptotic relation at high frequencies. Many of the estimates here of corner frequency and long-period level are tenuous, and those which were made with little confidence are represented by dashed lines in Figure 5. Occasionally we computed spectra for 256-second windows for those cases where the signal-to-noise ratio was adequate at lower frequencies, but for these cases the shape of the spectra was sufficiently similar to those

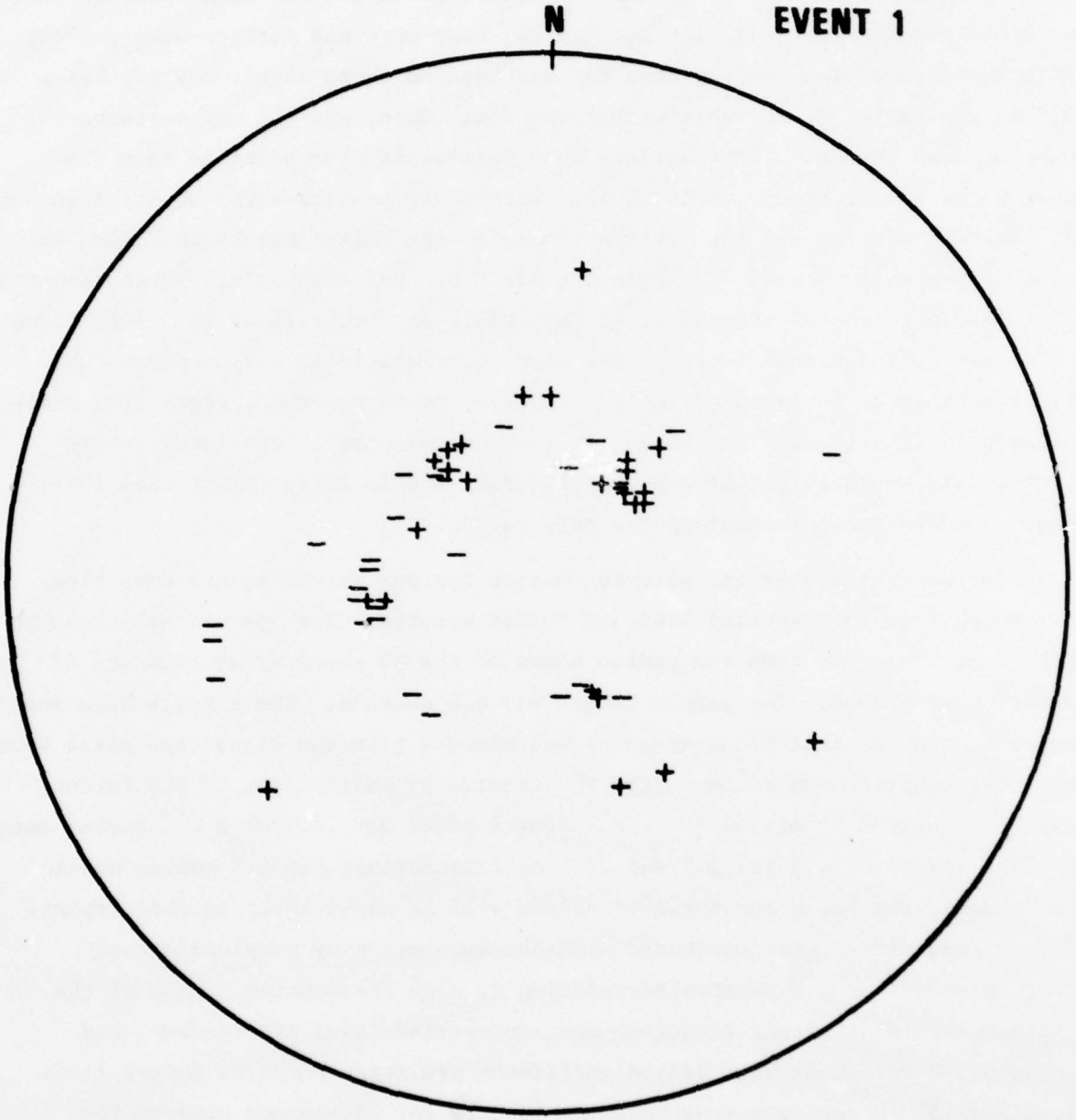

Figure 4. First motions for Baikal events in the lower half of the focal sphere (Wulff net).

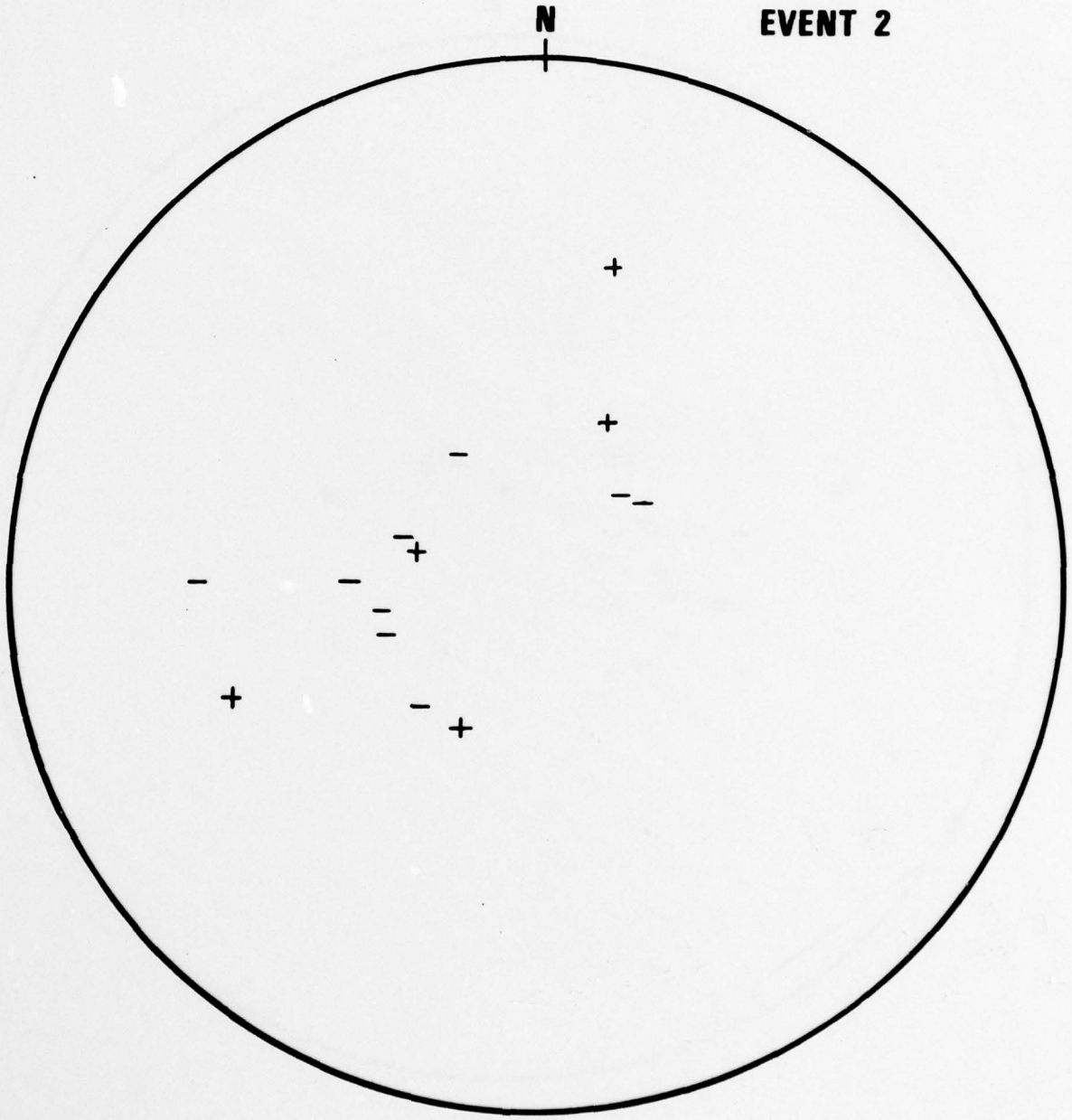

Figure 4 (cont.) First motions for Baikal events in the lower half of the focal sphere (Wulff net).

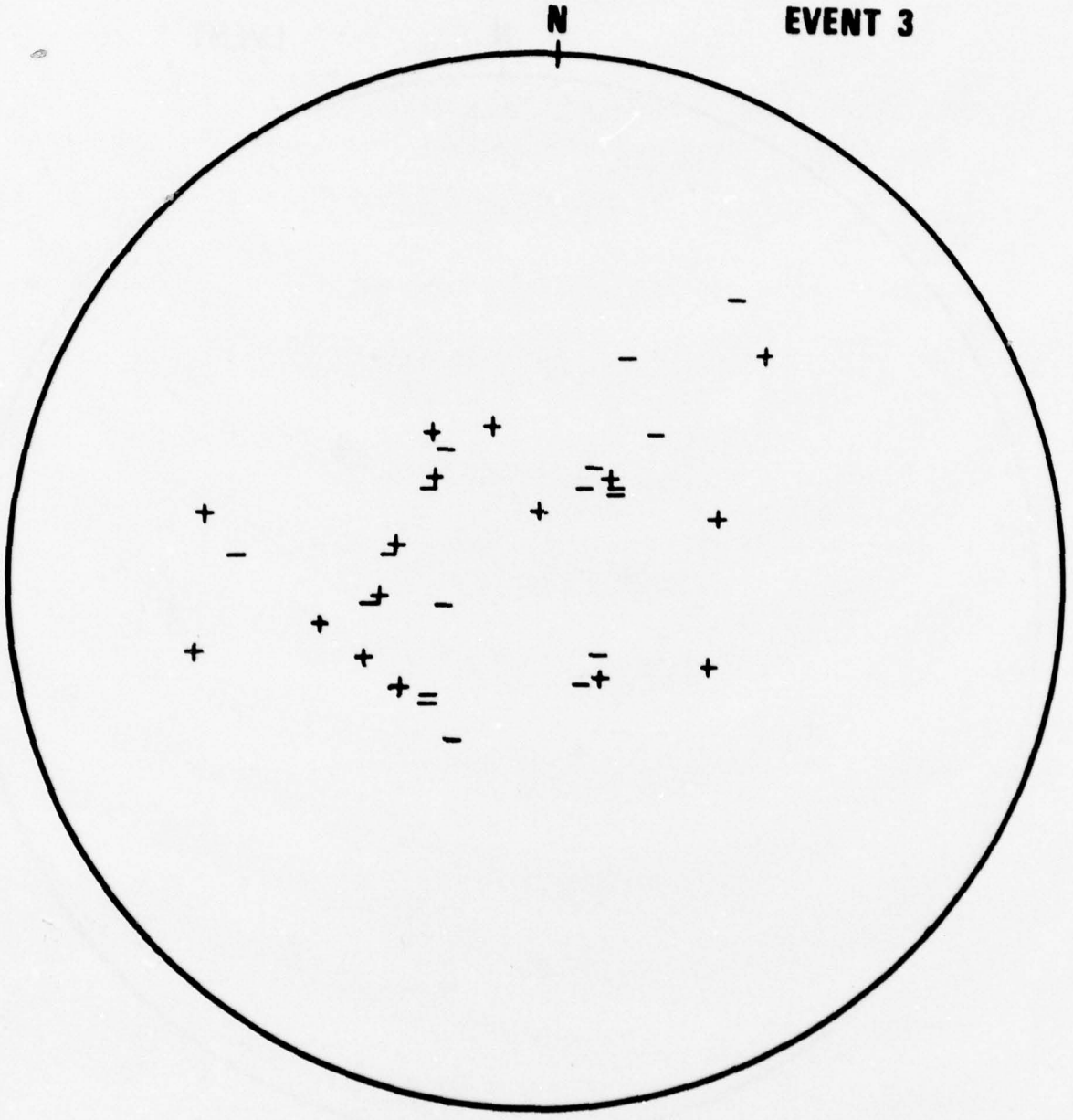

Figure 4 (cont.) First motions for Baikal events in the lower half of the focal sphere (Wulff net).

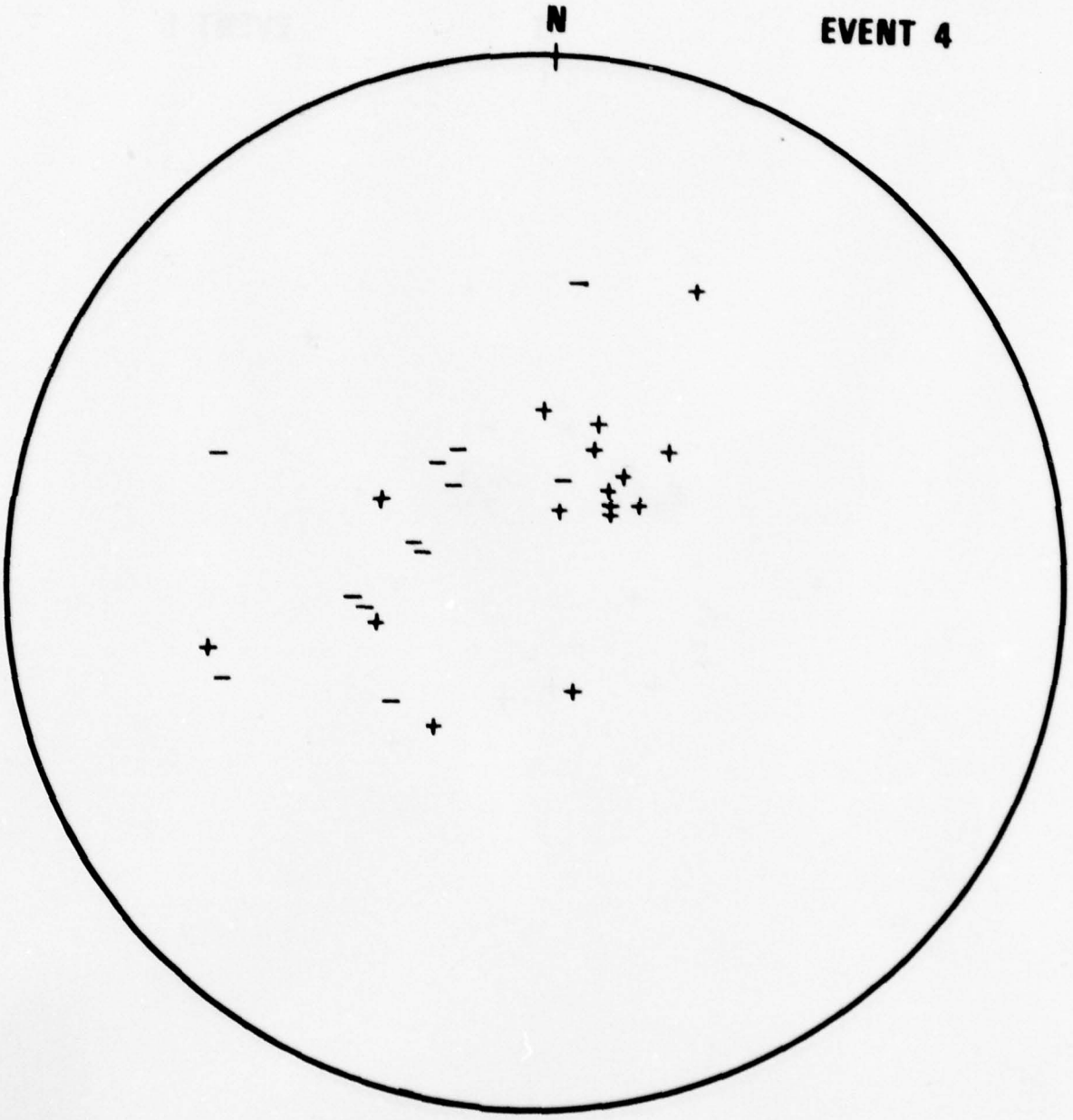

Figure 4 (cont.) First motions for Baikal events in the lower half of the focal sphere (Wulff net).

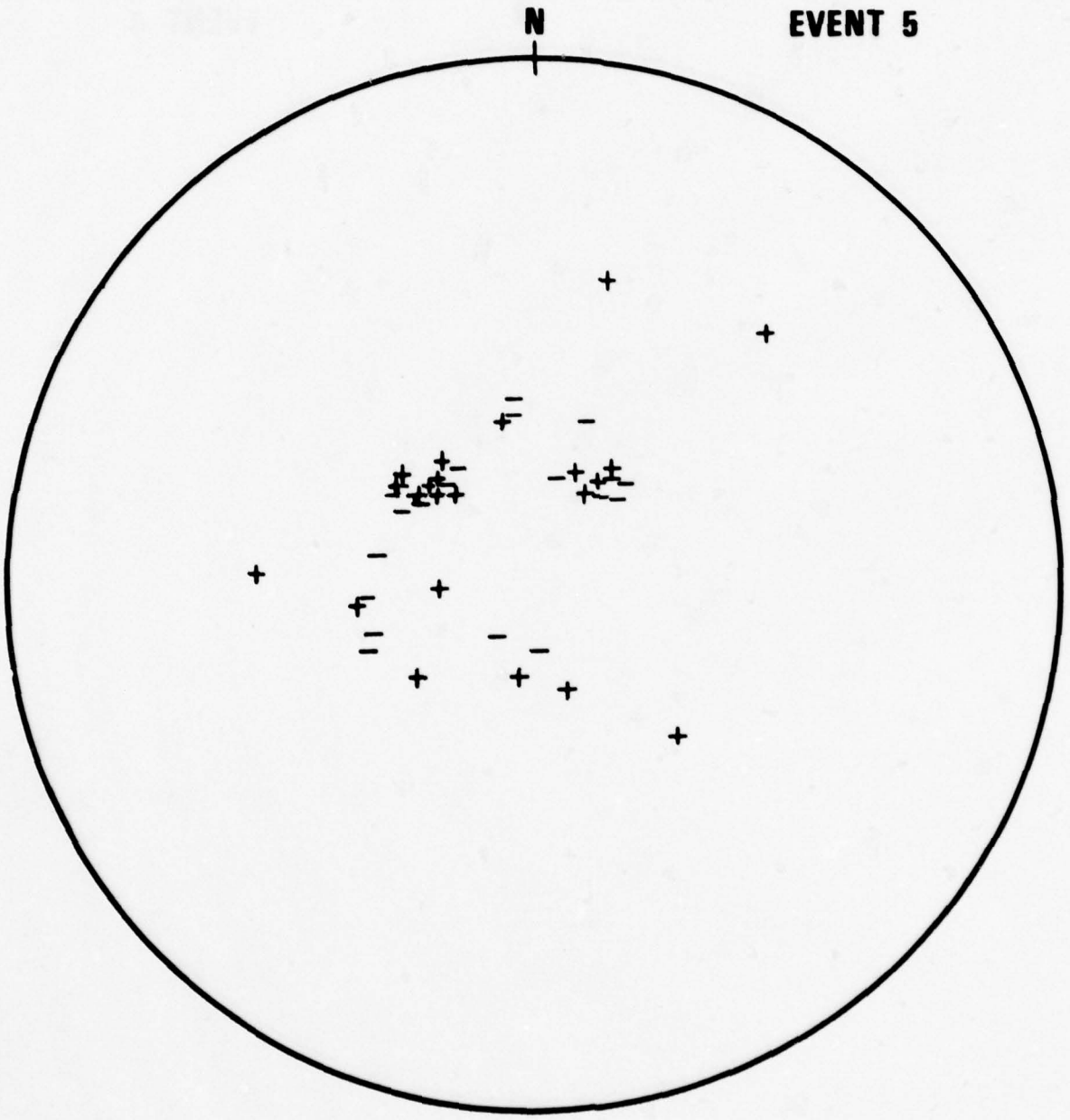

Figure 4 (cont.) First motions for Baikal events in the lower half of the focal sphere (Wulff net).

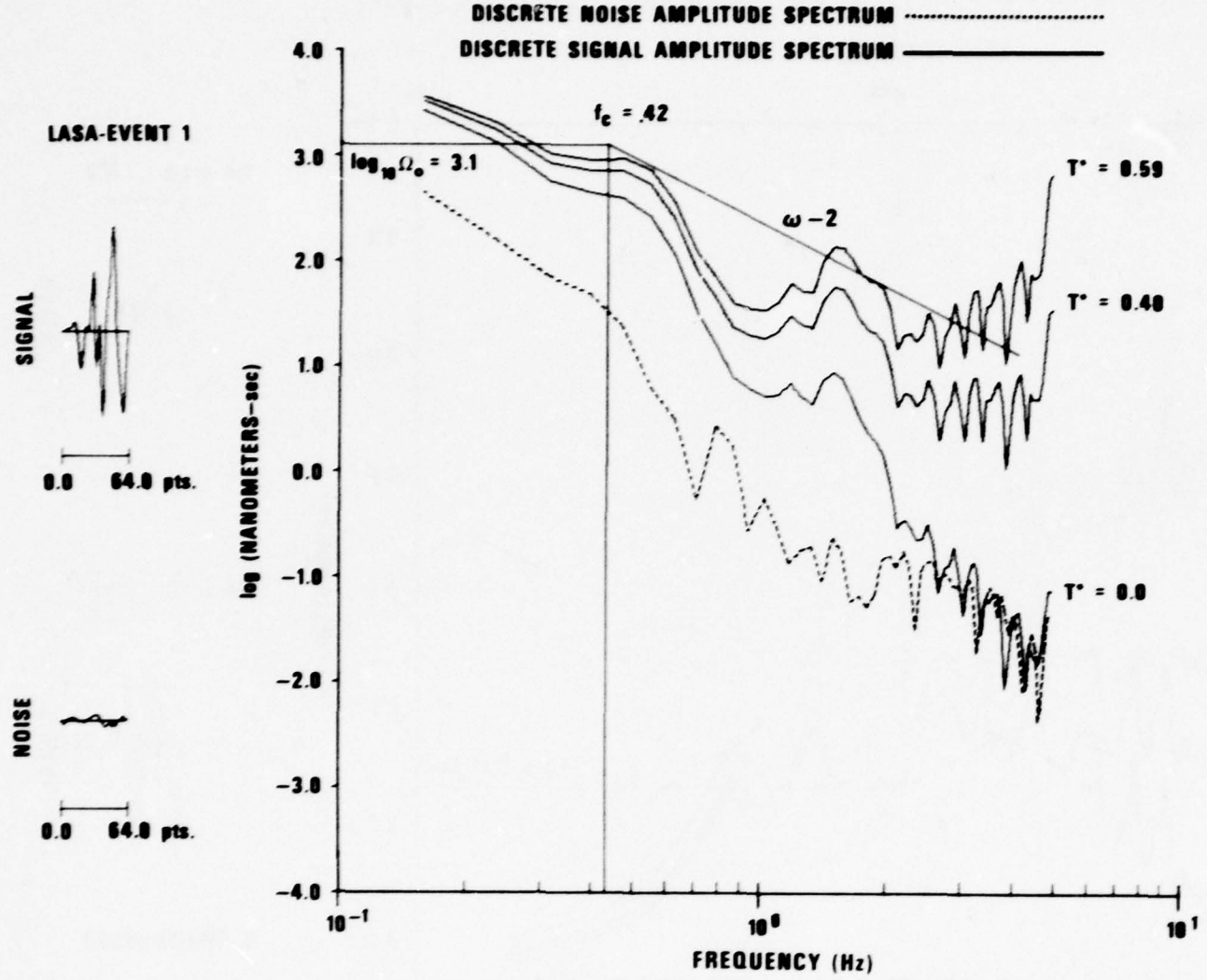

Figure 5. LASA A0 and NORSAR C3 subarray spectra of P waves from Baikal events with instrument response and attenuation removed.

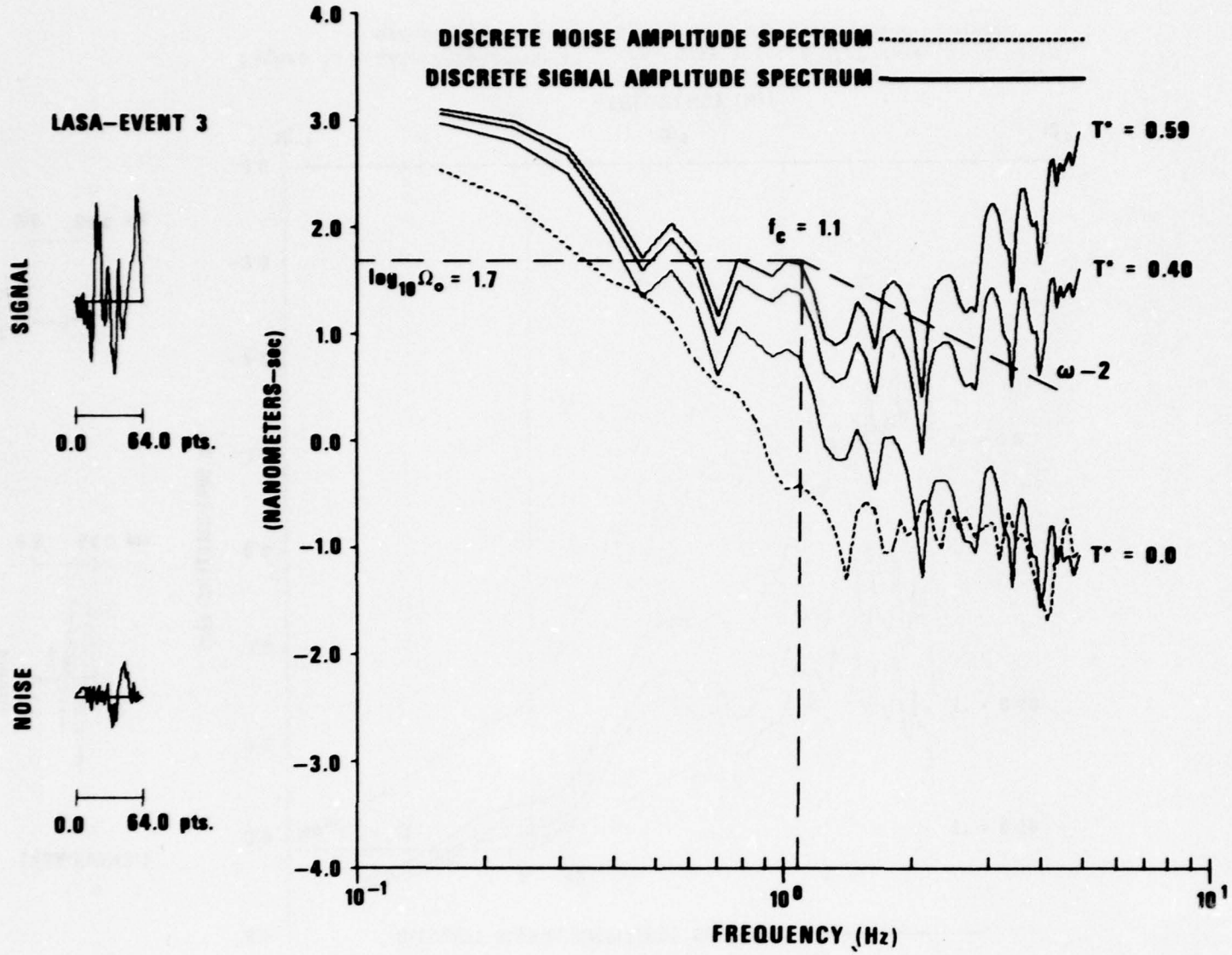

Figure 5 (cont.) LASA A0 and NORSAR C3 subarray spectra of P waves from Baikal events with instrument response and attenuation removed.

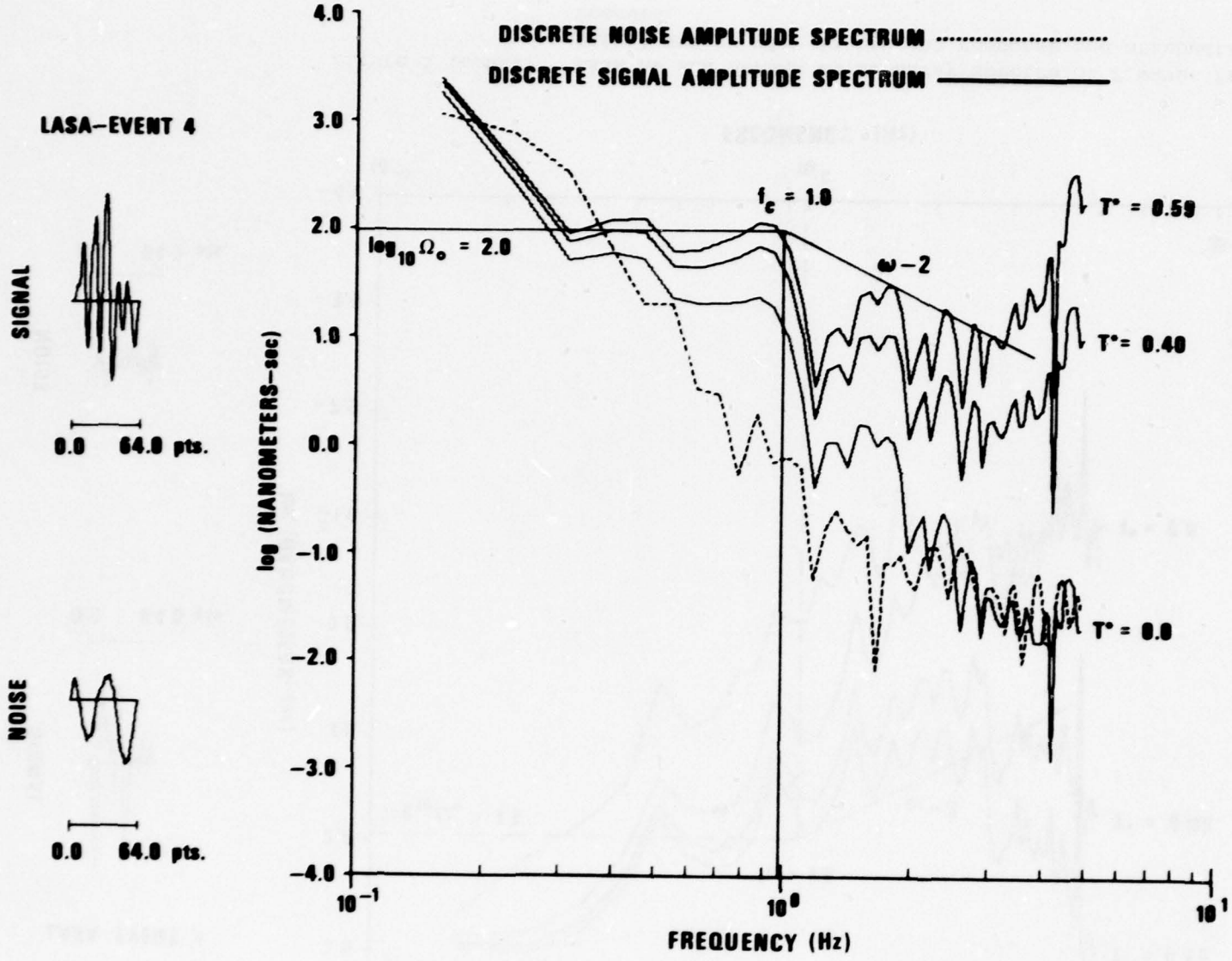

Figure 5 (cont.) LASA A0 and NORSAR C3 subarray spectra of P waves from Baikal events with instrument response and attenuation removed.

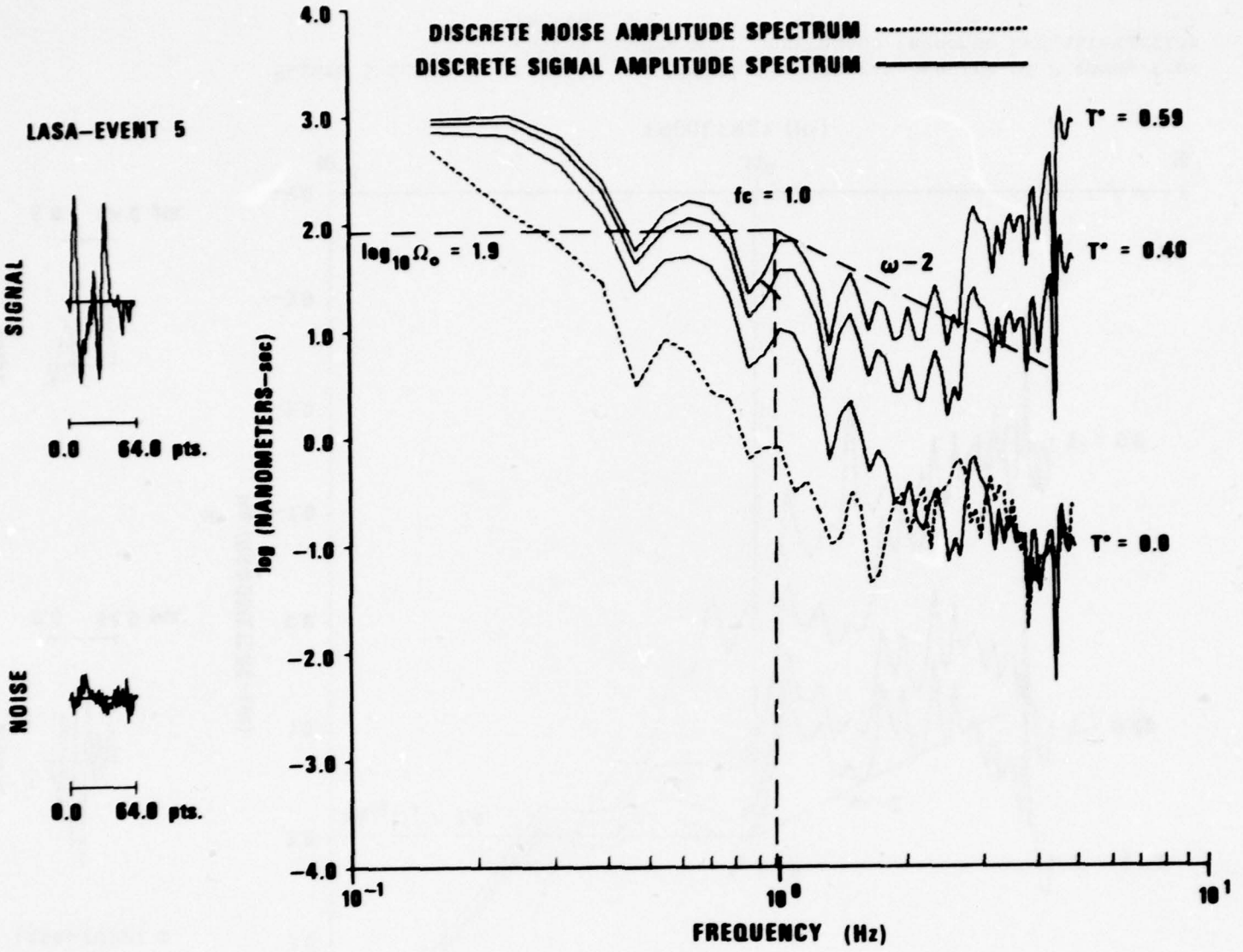

Figure 5 (cont.) LASA AO and NORSAR C3 subarray spectra of P waves from Baikal events with instrument response and attenuation removed.

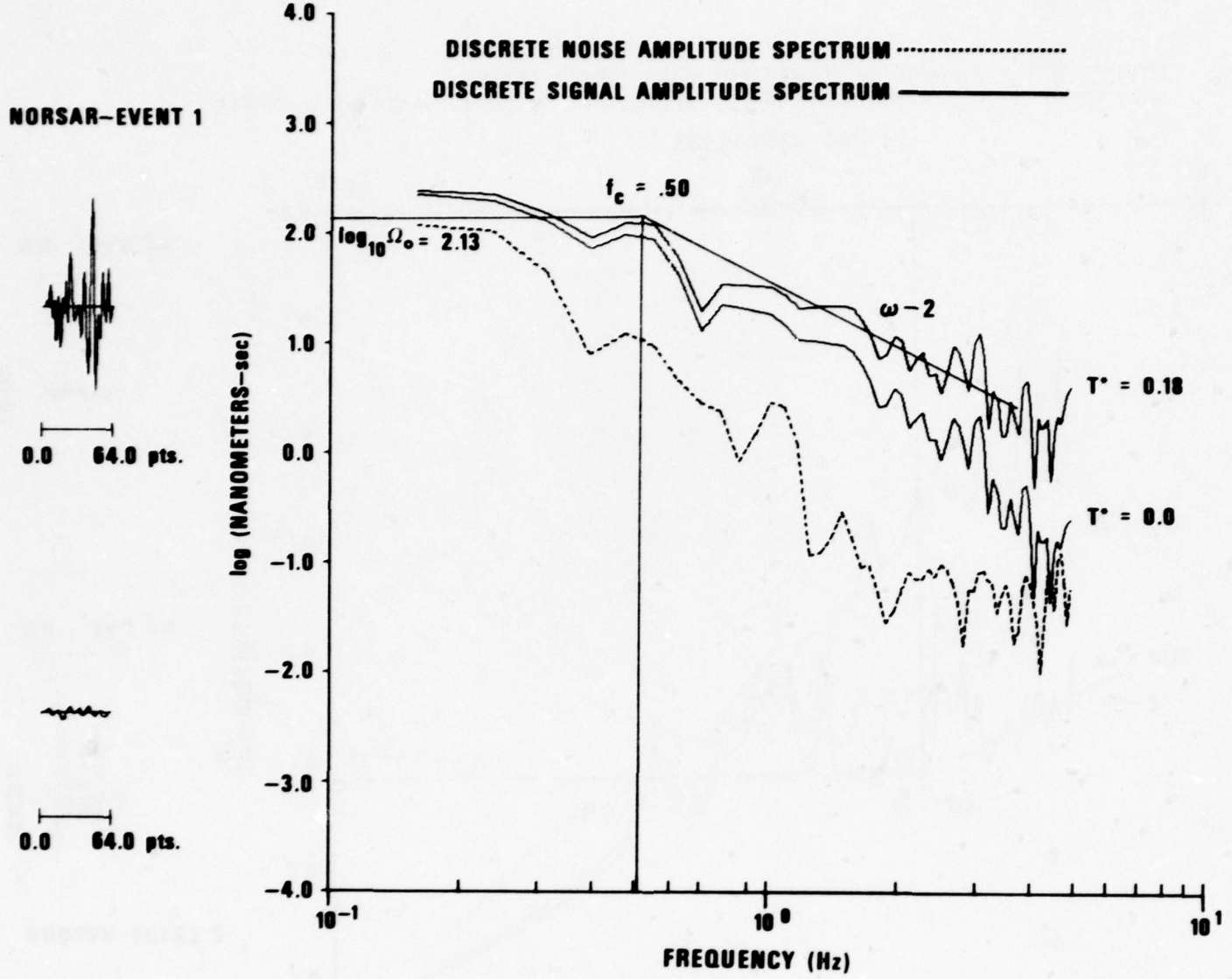

Figure 5 (cont.) LASA AO and NORSAR C3 subarray spectra of P waves from Baikal events with instrument response and attenuation removed.

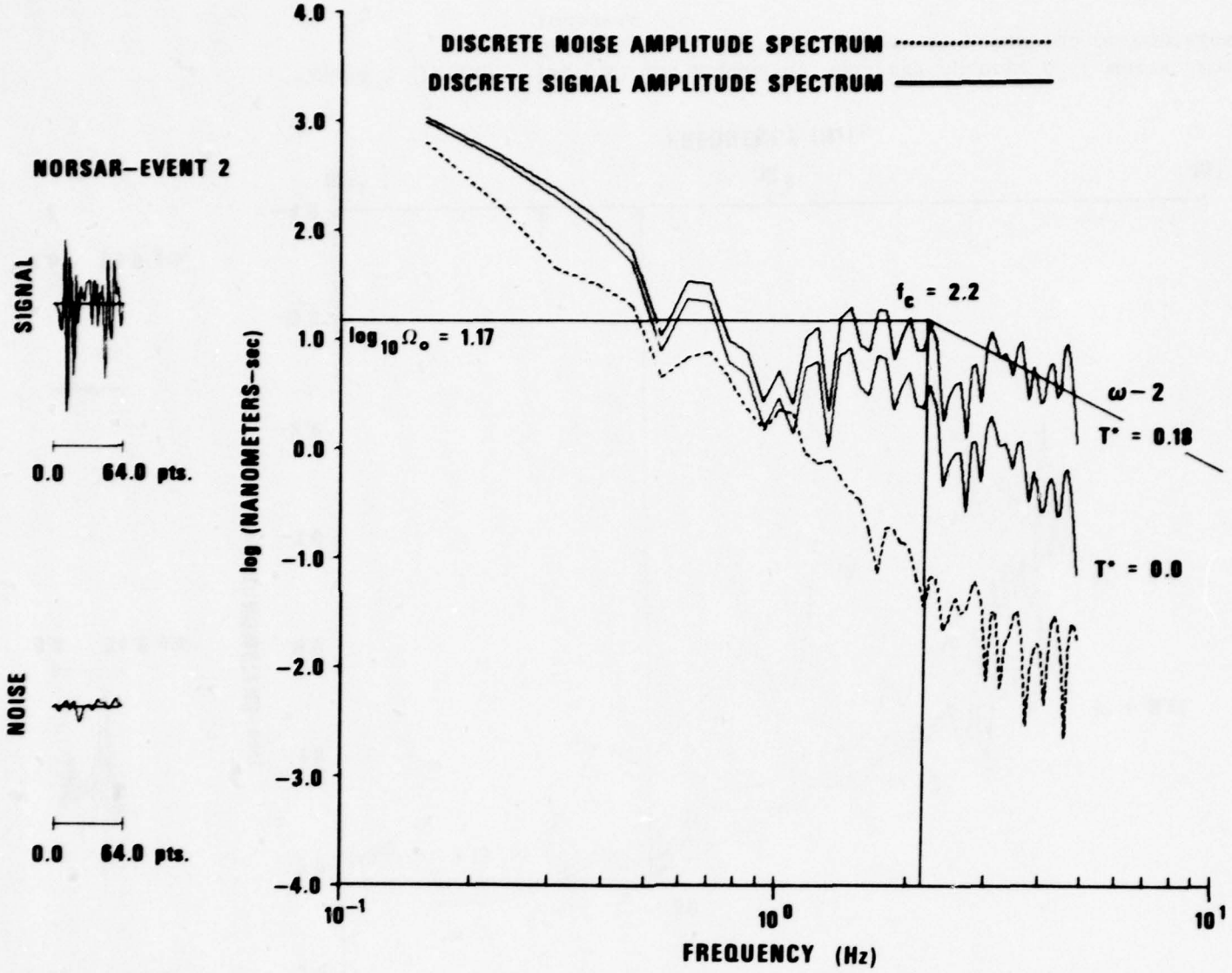

Figure 5 (cont.) LASA AO and NORSAR C3 subarray spectra of P waves from Baikal events with instrument response and attenuation removed.

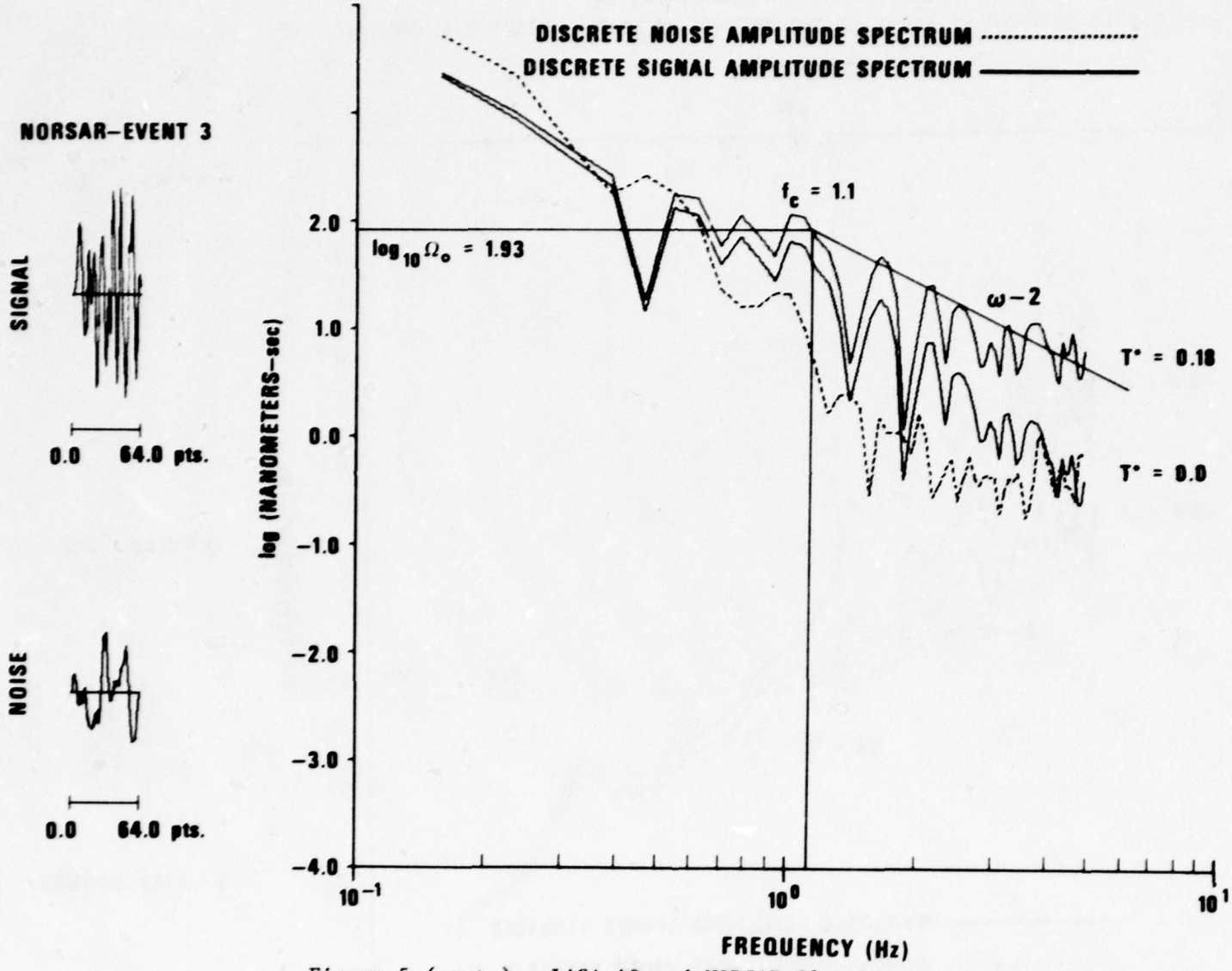

Figure 5 (cont.) LASA A0 and NORSAR C3 subarray spectra of P waves from Baikal events with instrument response and attenuation removed.

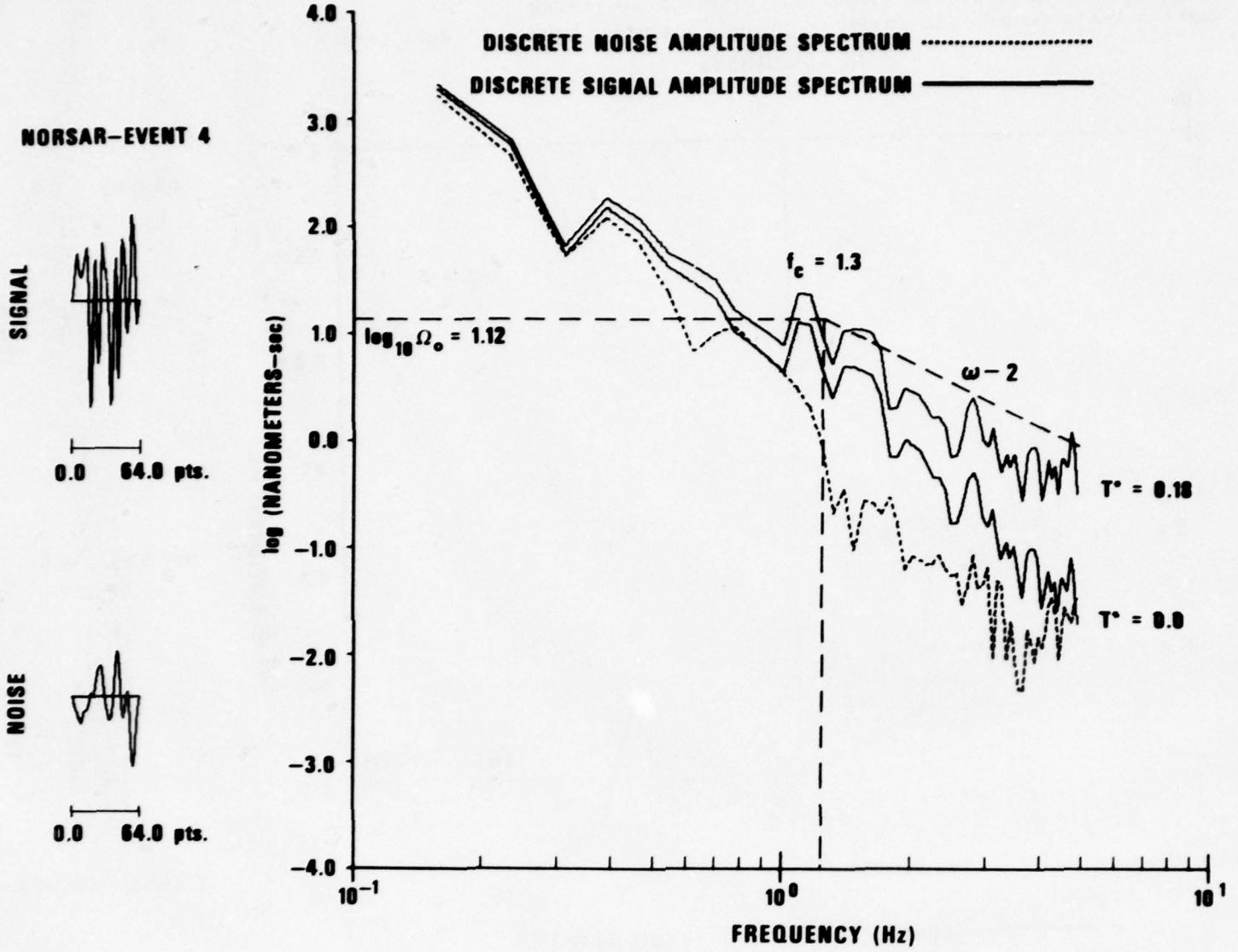

Figure 5 (cont.) LASA A0 and NORSAR C3 subarray spectra of P waves from Baikal events with instrument response and attenuation removed.

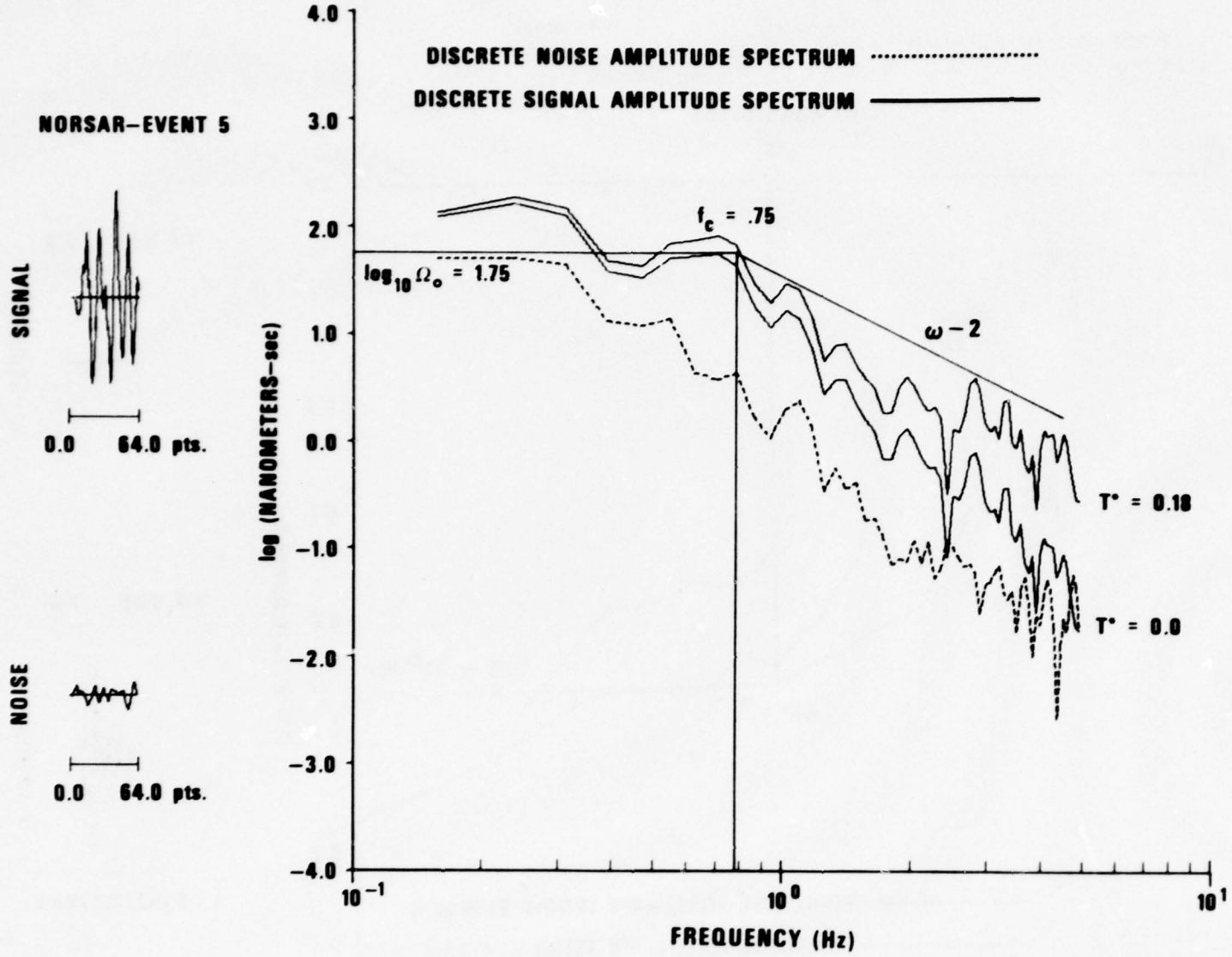

Figure 5 (cont.) LASA AO and NORSAR C3 subarray spectra of P waves from Baikal events with instrument response and attenuation removed.

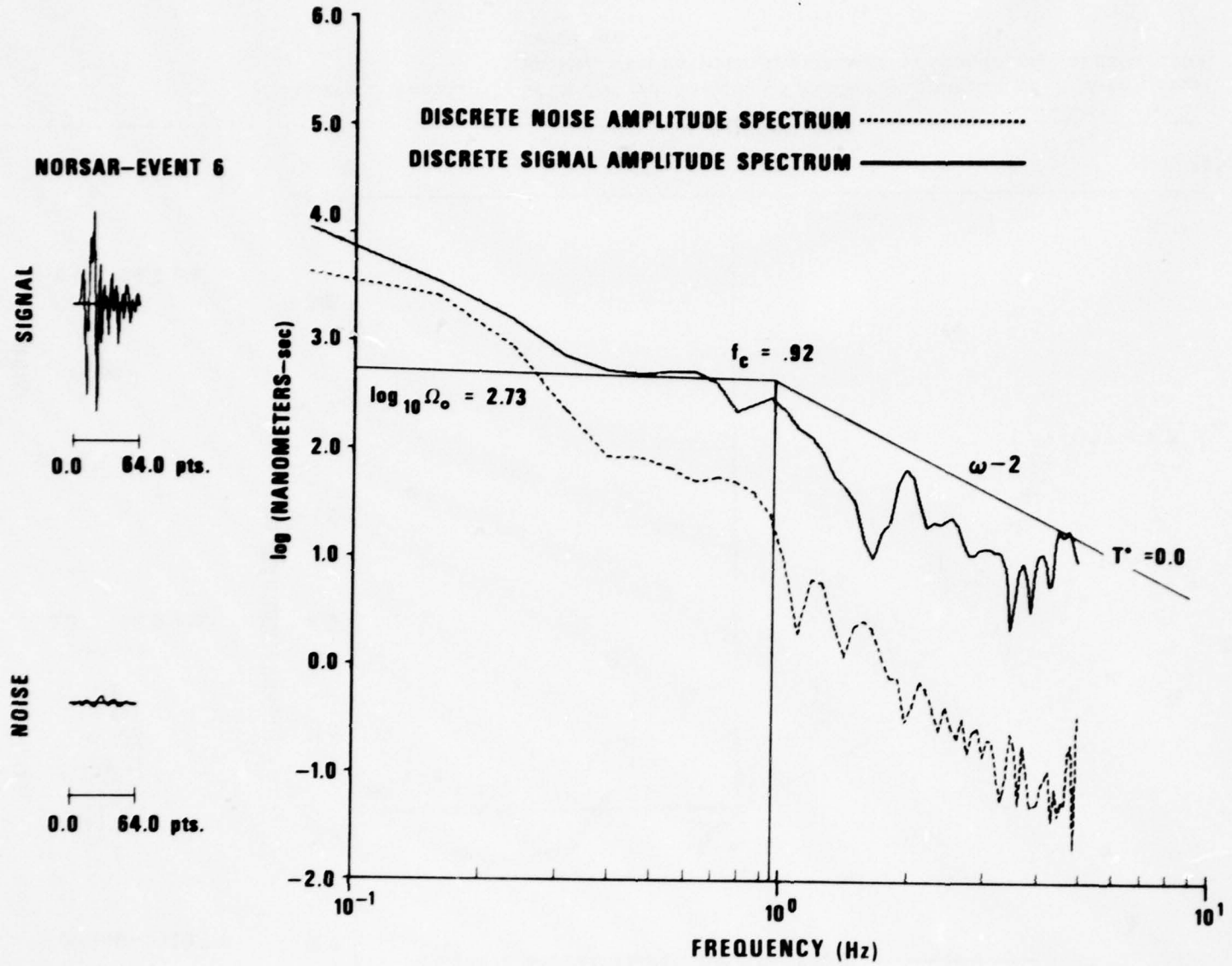

Figure 5 (cont.) LASA A0 and NORSAR C3 subarray spectra of P waves from Baikal events with instrument response and attenuation removed.

for the 6.4-second windows that have not shown them. Note that for some cases the signal-to-noise ratio was high down to low frequencies.

Seismic moment was calculated from the body-wave spectral displacement levels $|\Omega_o|$ estimated in Figure 5 at low frequencies using the relation

$$M_o = \frac{4\pi\rho\alpha^3 D|\Omega_o|}{R_{\theta\phi}}$$

where $R_{\theta\phi}$ was assumed to be unity due to lack of firm knowledge of the focal mechanism, values of $\rho\alpha^3$ from Table I appropriate to the source depth were used, and the divergence factor D was applied (Ben-Menahem et al., 1965). A graph of moment versus corner frequency is shown in Figure 6. Our events fall close to or between the constant stress drop lines of Hanks and Thatcher (1972), indicating that our events are of intermediate stress drop.

We attempted to find the LR radiation pattern for each event by plotting the antilogs of the M_s values for each event as listed in Table IV. The results from the event with the largest M_s, event 1, are shown in Figure 7. The maximum antilog of M_s for the event plots on the outer circle and all the other antilog values for the event are scaled linearly between the center of the plot and the radius of the circle. The observed distribution of amplitudes does not obviously conform to any quadripole radiation pattern, which is probably due to varying propagation effects coupled with the large epicentral distances and the small magnitude of events studied. The scatter of data points for all the events was so poor that no attempt was made to find the best-fitting LR radiation patterns.

Propagation Effects

We measured relative mantle attenuation along the paths from the Baikal events to LASA and NORSAR, the only two sites for which we had short-period digital data. Our measurement of attenuation is the factor t*, which is the

---

Ben-Menahem, A., S. Smith, and T. Teng (1965). A procedure for source studies from spectrums of long-period seismic body waves, Bull. Seism. Soc. Am., 55, 203.

Hanks, T., and W. Thatcher (1972). A graphical representation of seismic source parameters, J. Geophys. Res., 77, 4393.

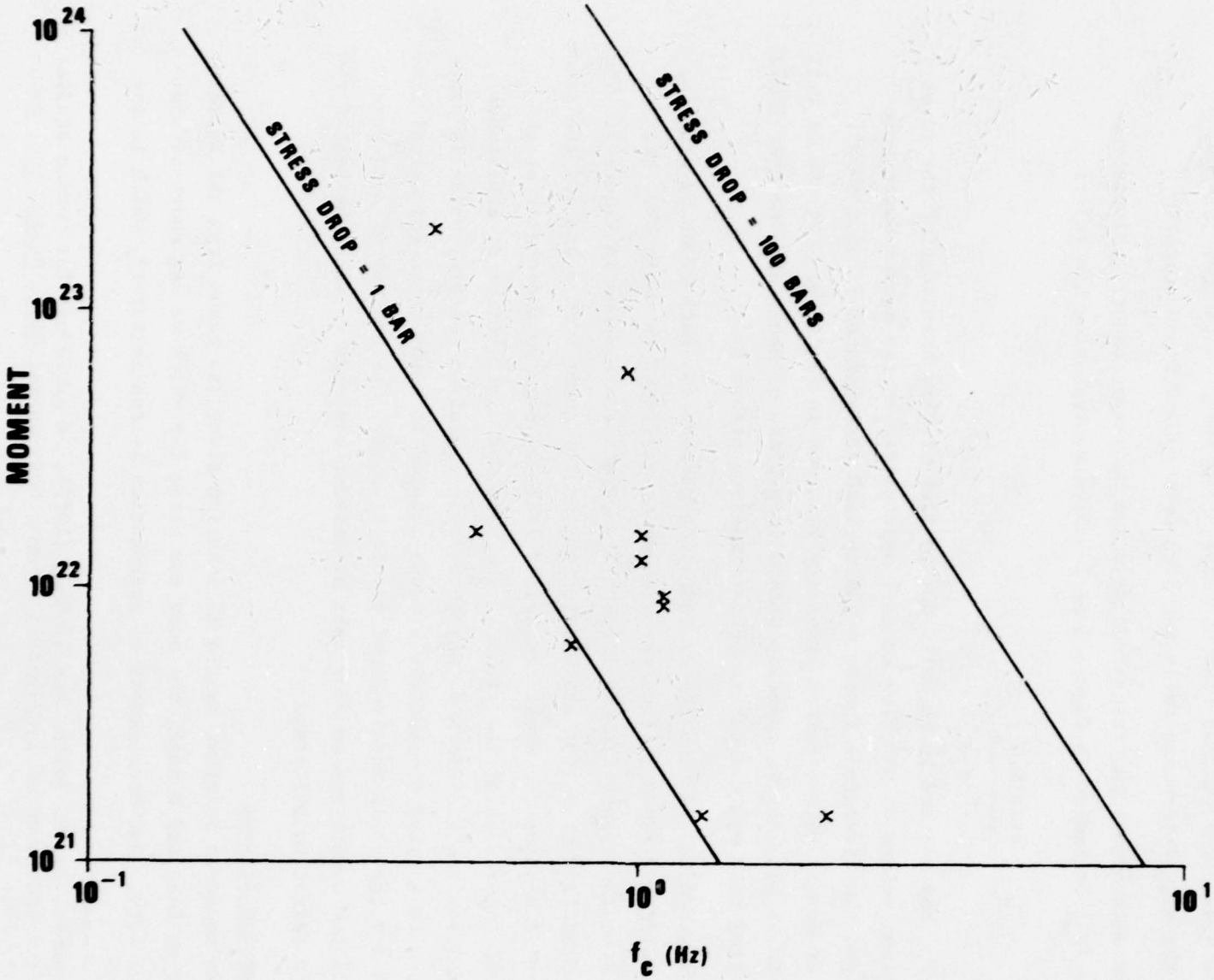

Figure 6. Seismic moment versus corner frequency for Baikal events from LASA and NORSAR P recordings.

TABLE IV

Magnitude Data for Baikal Events

Event 1

Station	Δ	m_b	M_s
ALQ	79.5	5.49	5.45
CHG	41.7	5.46	
COL	40.7	4.97	5.34
CTA	78.6		5.40
EIL	65.1		5.58
EIL	65.1		5.38
JER	63.2	4.92	5.27
KBL	42.5	4.99	
KIP	65.9	5.95	
KON	53.2	5.29	5.65
LAO	69.0	5.85	
MAT	22.0	4.60	
NAO	51.6	5.34	
NIL	40.9	5.68	
NOR	40.6	4.76	
NUR	47.1	5.34	
OGD	81.5		5.76
PUE	47.0	4.96	5.33
SHL	38.2	5.82	
TOL	74.2	5.40	5.74
AVERAGE		5.30	5.49

EVENT 2

Station	Δ	m_b	M_s
ALQ	79.5	4.20	3.82
CHG	41.8	4.03	3.62
CTA	80.4		3.77
COL	40.8	4.48	
EIL	63.2	4.89	3.19
FBK	40.7		3.50
KBL	41.1	4.53	
NAO	49.7	5.16	3.95
NIL	39.6	4.07	
NUR	45.1	4.68	
OGD	80.7	5.16	-4.25
QUE	45.6	4.13	4.07
SHL	37.9	3.90	
TLO	72.2		4.33
AVERAGE		4.48	3.77

Note: negative M_s values reflect a noise measurement when no signal is visible

EVENT 3

Station	Δ	m_b	M_s
AAE	70.1		4.58
ATU	57.4	5.53	
BUL	99.4	5.00	
HLW	58.7	5.23	4.40
JER	54.9	4.80	4.72
KOD	49.0	5.46	5.21
LAO	76.2	5.02	4.50
MAT	26.9	4.24	4.03
MSH	37.2	5.06	4.60
NAI	79.5	4.80	4.92
NAO	48.5	4.21	5.31
NDI	32.9	4.88	4.55
NIL	31.0	4.58	4.91
NUR	43.1	4.70	5.04
POO	43.1	4.97	
QUE	37.2		4.75
SHI	46.0	5.37	5.05
SHL	29.8	5.24	
TAB	44.0		4.24
TRI	57.3	4.77	5.51
UME	43.4	4.68	5.15
AVERAGE		4.92	4.79

Event 4

Station	Δ	m_b	M_s
ALP	40.5		-3.52
ALQ	79.4	4.73	4.51
CHG	41.7	4.57	3.89
COL	40.7	5.17	
CTA	78.8	4.91	4.27
EIL	65.0	5.76	4.60
JER	63.1	4.91	4.30
KBL	42.4	5.36	4.34
DIP	66.0		4.37
KON	50.0		4.75
KON	50.0		4.55
LAO	68.9	5.48	
NAO	51.5	4.96	4.55
NIL	40.8	4.75	
NUR	47.0		4.64
OGD	81.4	4.84	
QUE	46.9	4.59	4.50
SHL	38.2	4.58	
TLO	74.1	4.76	4.32
TLO	74.1		4.57
AVERAGE		4.95	4.37

Event 5

Station	Δ	m_b	M_s
ALP	42.5		3.32
ALQ	81.3	5.04	3.79
CHG	40.1	4.51	3.68
CTA	80.4		4.09
DAG	43.9	4.70	
EIL	61.6		4.23
KIP	69.4		3.89
LAO	70.6	5.31	3.72
MAT	24.4		4.43
NAO	49.3	5.30	4.66
NIL	37.6	5.14	4.35
OGD	81.9	5.28	4.32
TLO	71.7		4.44
AVERAGE		5.04	4.08

Event 6

Station	Δ	m_b	M_s
ALQ	79.1		-2.54
ANMO	79.1	4.67	-3.56
CTAO	85.1	5.11	
GUMO	52.7		-2.86
KIP	71.0		-2.76
KON	46.0		-2.88
MAIO	41.5	4.25	3.28
MAT	29.2		-2.37
OGD	78.1		-2.96
AVERAGE		4.68	3.28

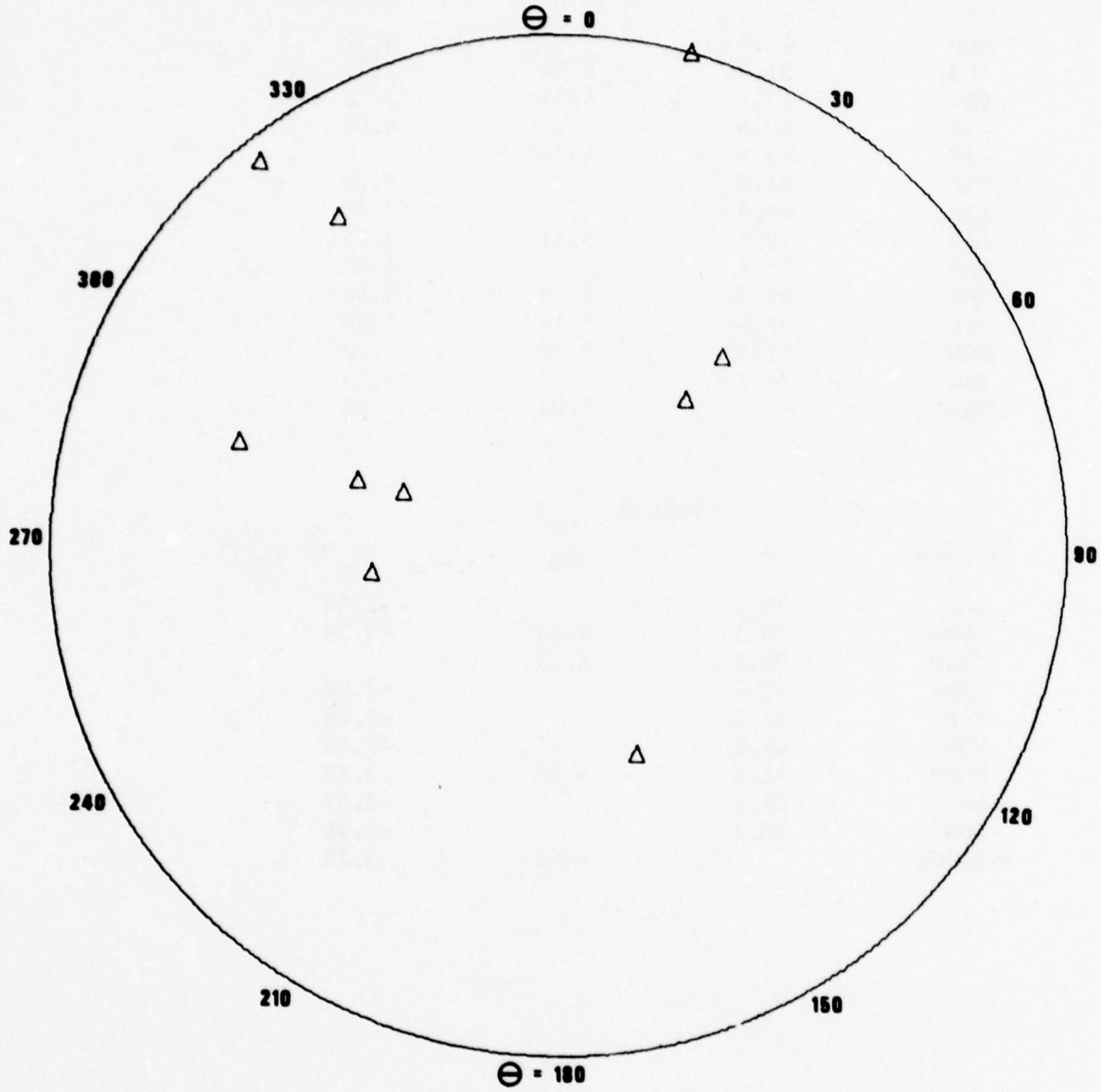

Figure 7. Observed LR amplitudes (T = 20 sec) for Baikal event 1.

travel time along the ray path divided by the average attenuation factor Q.

We determine t* by first normalizing and then summing the t*=0 spectra shown in Figure 5 for each of the two paths: Baikal to LASA and Baikal to NORSAR. These averages are shown in Figures 8 and 9 and represent the average relative ground displacement density spectra at the two sites. If we assume that the source spectra has an f^{-2} fall off at high frequencies, then

$$F(f) \simeq S \cdot f^{-2} \cdot e^{-\pi f t^*}$$

for frequencies above the corner frequency where F(f) is the observed spectrum (corrected for seismograph response), S is the source spectrum scale constant, and f is frequency in Hz. Then after taking the natural log of this equation

$$\ln[F(f)] + 2 \cdot \ln(f) = -\pi t^* f + \ln(S)$$

If we plot $\ln[F(f)] + 2 \cdot \ln(f)$ versus frequency for each path, as shown in Figures 10 and 12, the slope of the graph is $-\pi t^*$. We calculated the slope in the frequency range 1.0 to 2.5 Hz, where the signal-to-noise ratio was highest, and presumably beyond the corner frequency so that the high-frequency asymptotic slope of f^{-2} characterizes the source spectrum. Figure 5 shows that some of the corner frequencies are above 1 Hz, so the data may not be well fitted by the above equation; but if a higher frequency range were used, we would seriously contaminate the average spectra with background noise. The effect of using spectral estimates at frequencies below the corner frequency is to bias the slope t* toward a lower value than the actual one. Thus t* results here are not as reliable as needed to confidently characterize the attenuation along the two paths. Similarly, the equation for a source spectra with an f^{-3} fall off is

$$\ln[F(f)] + 3 \cdot \ln(f) = -\pi t^* f + \ln(S)$$

If we plot the left-hand side of this relation versus frequency for each path as shown in Figures 11 and 13, the slope of the graph is again $-\pi t^*$; but t* is now based on an assumed f^{-3} source spectrum.

The t* values for an f^{-2} source model are $.59 \pm .40$ for the Baikal to LASA path and $.18 \pm .07$ for the Baikal to NORSAR path. The t* values for an f^{-3} source model are $.40 \pm .16$ for the Baikal to LASA path and $-.00 \pm .07$ for the Baikal to NORSAR path. Separate t* values were calculated for event 6 since it lies a few degrees to the north of the rift zone and because it is

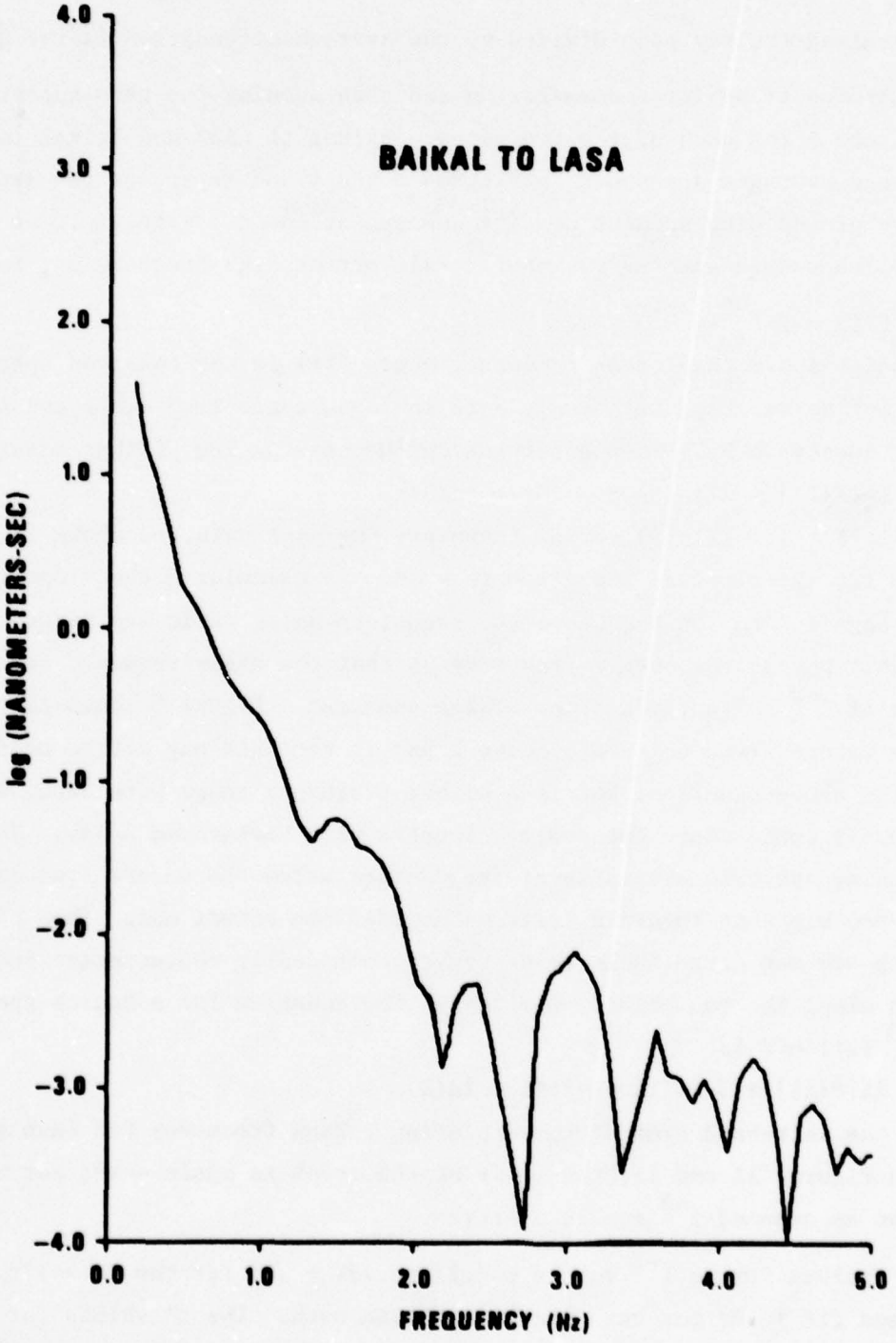

Figure 8. Average of spectra for the path Baikal to LASA for events 1 through 5.

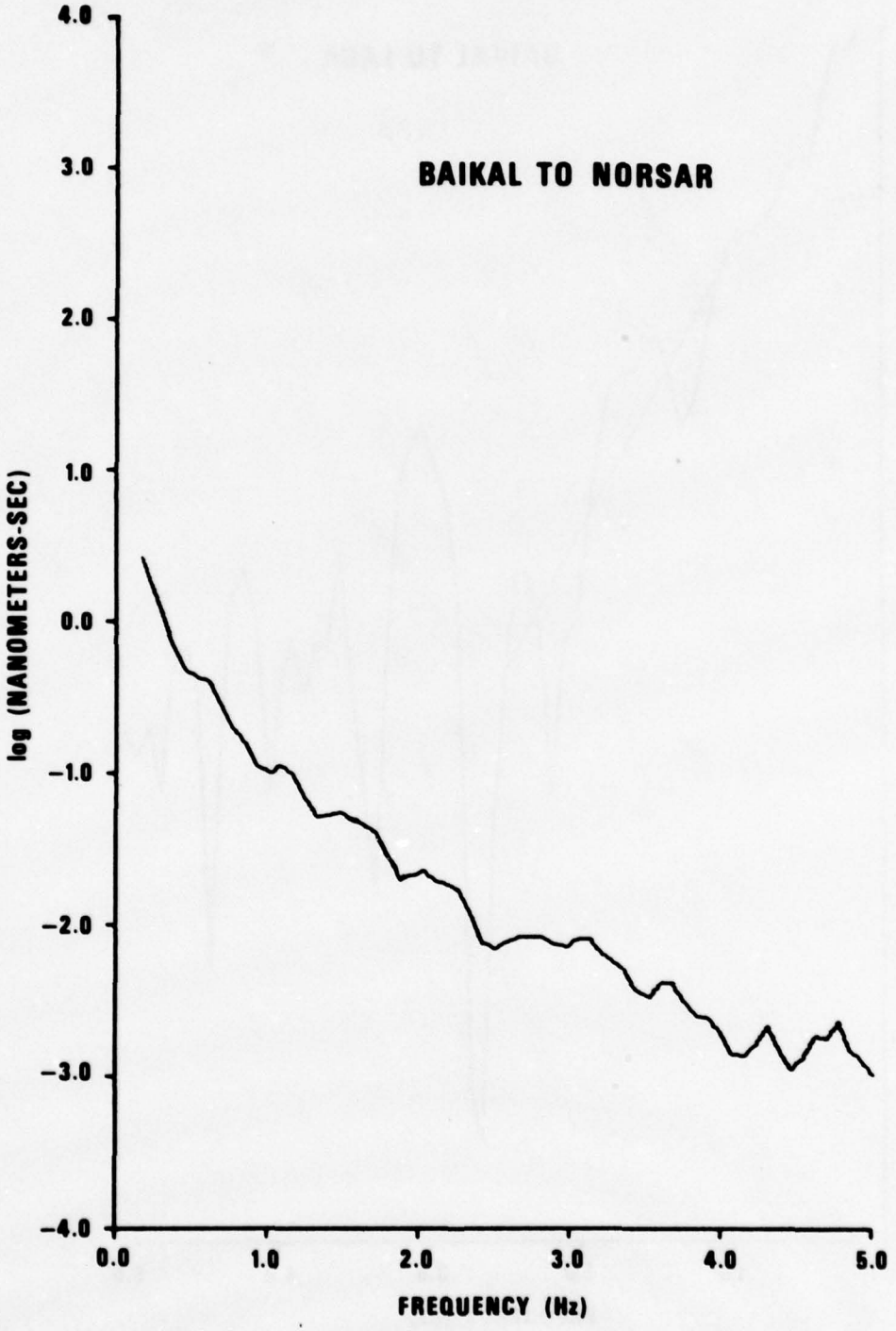

Figure 9. Average of spectra for the path Baikal to NORSAR for events 1 through 5.

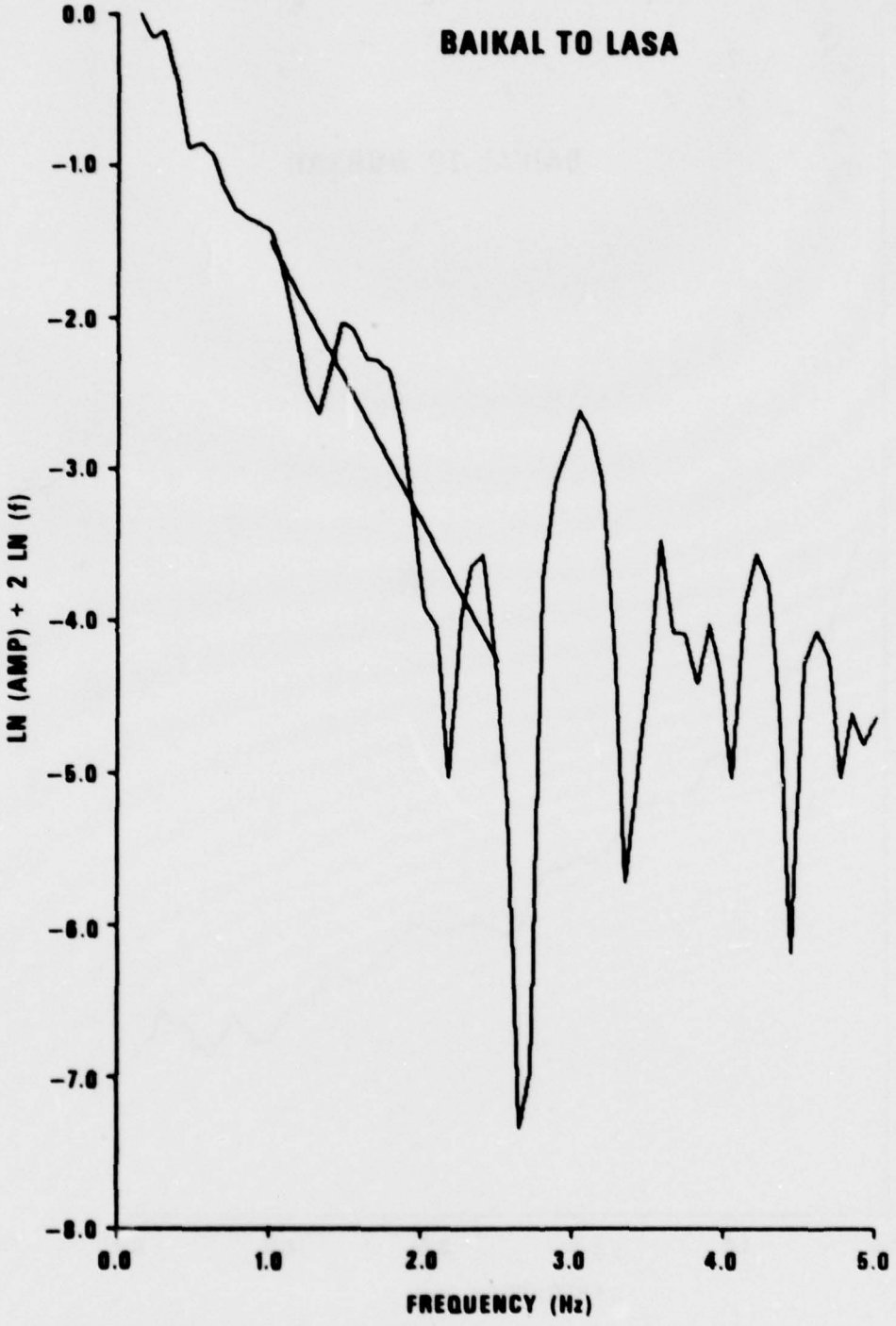

Figure 10. Ln (F) + 2 ln (f) versus frequency for the path Baikal to LASA.

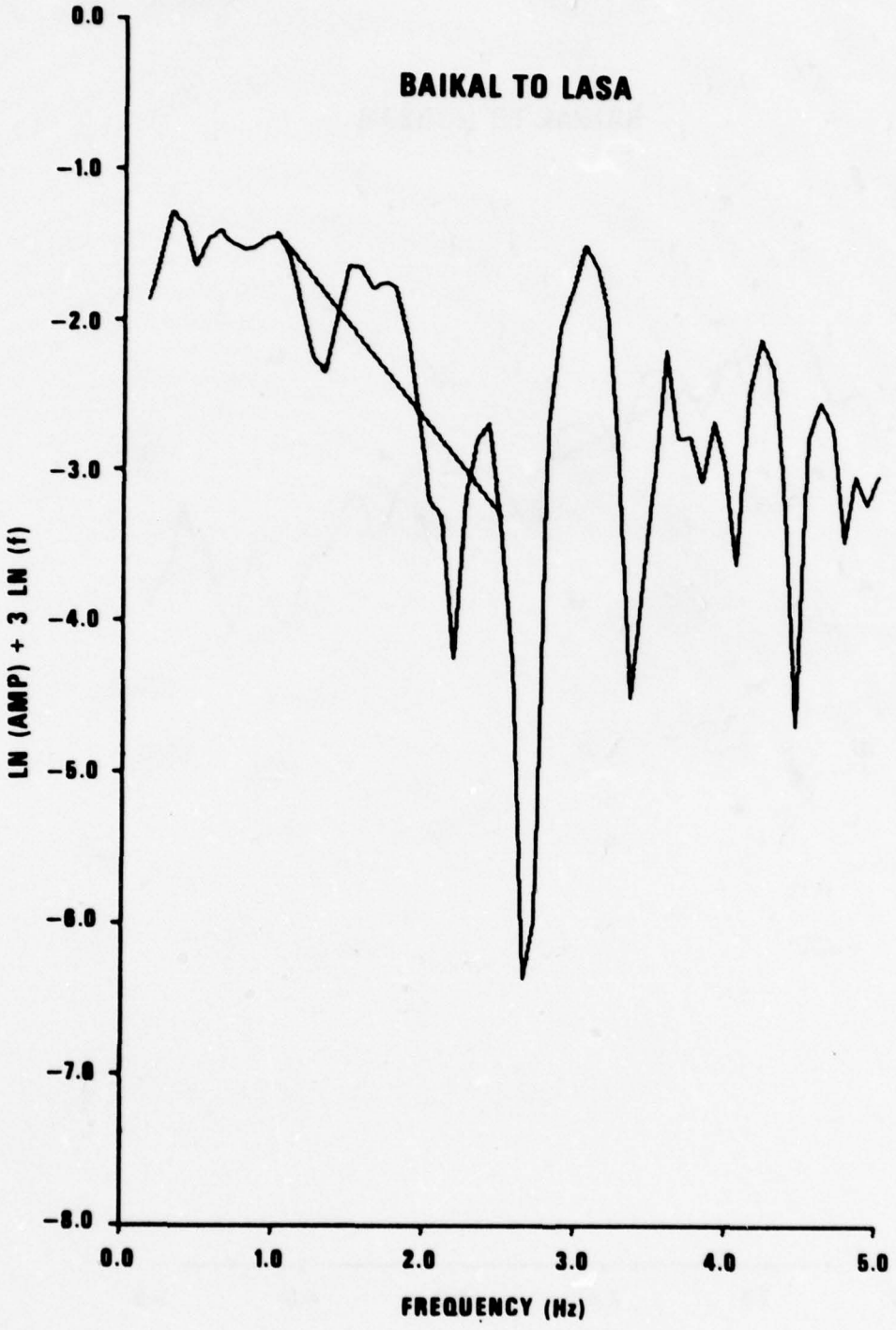

Figure 11. Ln (F) + 3 ln (f) versus frequency for the path Baikal to LASA.

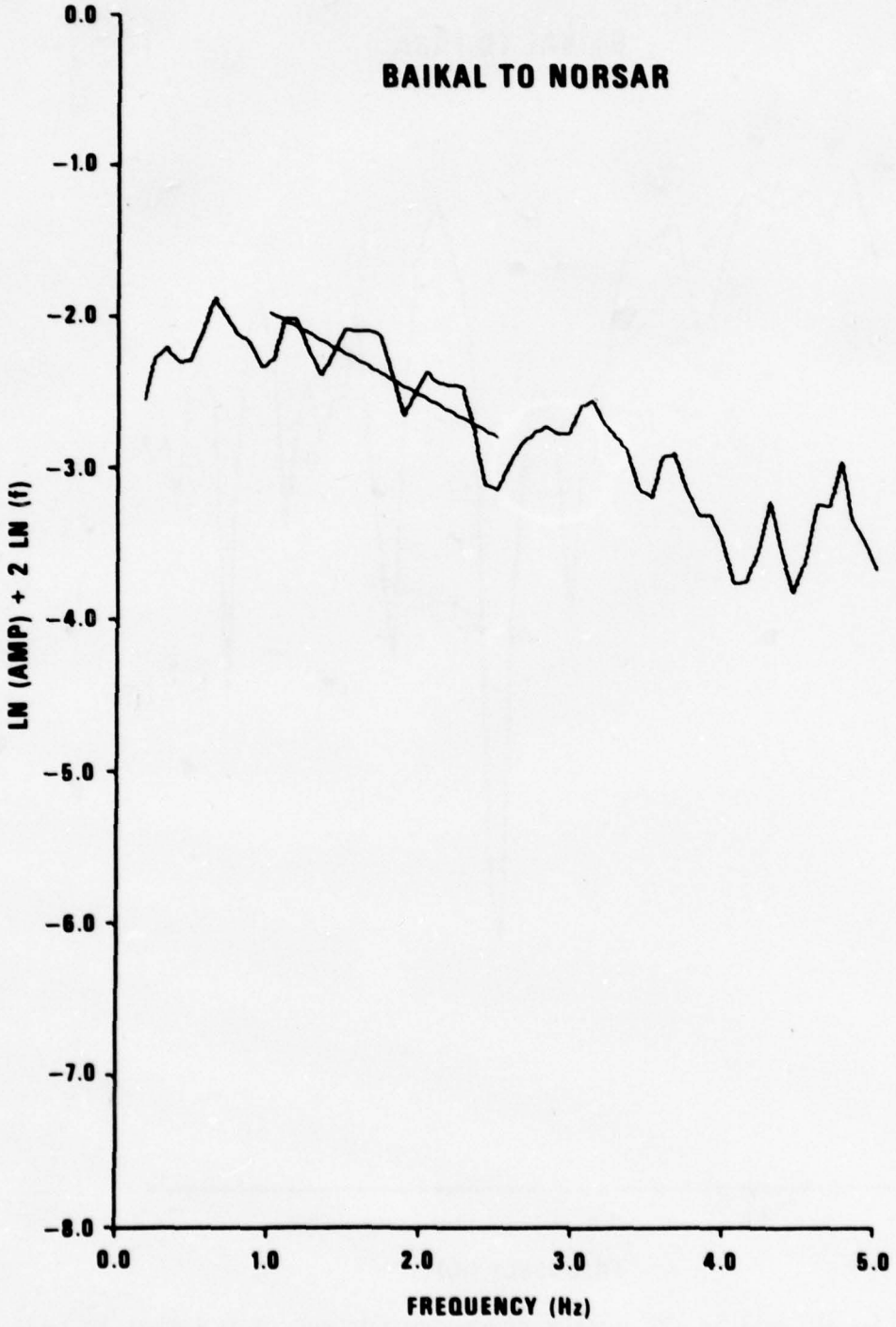

Figure 12. Ln (F) + 2 ln (f) versus frequency for the path Baikal to NORSAR.

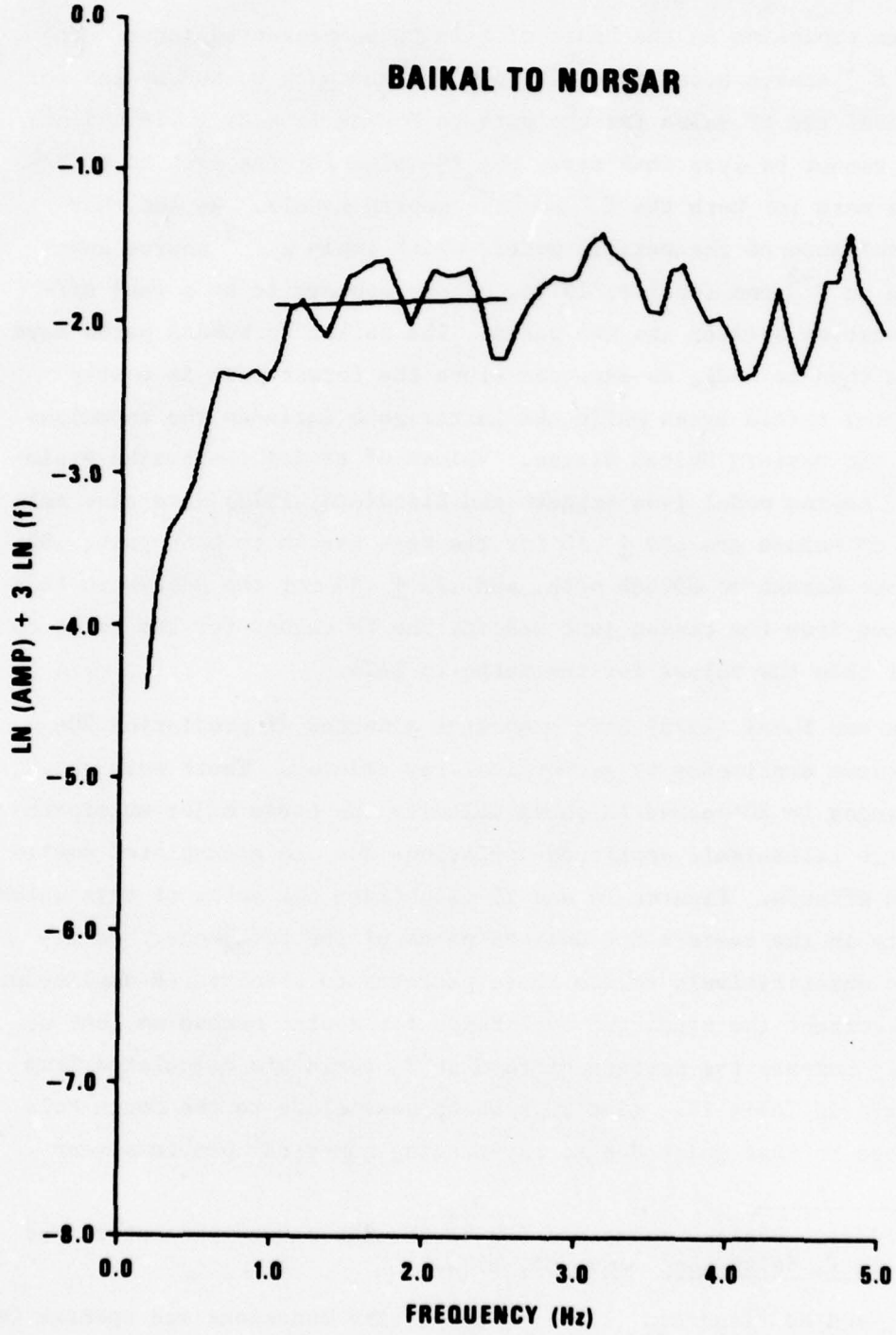

Figure 13. Ln (F) + 3 ln (f) versus frequency for the path Baikal to NORSAR.

presumed to be an explosion on the basis of data to be presented later. The t* value for an f^{-2} source model is $-.01 \pm .19$ for the path to NORSAR and for an f^{-3} source model the t* value for the path to NORSAR is $-.20 \pm .18$. Since the value of t* cannot be less than zero, the t* value for the path to NORSAR is assumed to be zero for both the f^{-2} and f^{-3} source models. We add that there is a predominance of theoretical models which imply a f^{-3} source spectrum rather than an f^{-2} one (Geller, 1976). There appears to be a real difference in attenuation between the two paths. The Baikal to NORSAR paths have less attenuation than to LASA, as expected since the former path is mostly through continental shield areas while the latter path includes the anomalous upper mantle of the western United States. Values of t* for the Kazakh explosions for an f^{-2} source model (von Seggern and Blandford, 1972) were also calculated. These t* values are $.16 \pm .10$ for the East Kazakh to LASA path, $.05 \pm .08$ for the East Kazakh to NORSAR path, and $.23 \pm .10$ for the MILROW to LASA path. As expected from the reason just stated, the t* values for the paths to NORSAR are lower than the values for the paths to LASA.

von Seggern and Sobel (1975) have presented a method of predicting 20-second Rayleigh-wave amplitudes by geometrical ray tracing. Their work shows that lateral changes in 20-second LR phase velocity can cause major multipathing and also large teleseismic amplitude variations due to accumulated small-scale refraction effects. Figures 14 and 15 illustrate the paths of rays which result for events in the eastern and western parts of the rift zone. No attempt is made to quantitatively relate these patterns to observed LR amplitudes since we cannot correct the predicted amplitudes for source mechanism, but we can qualitatively compare the pattern of rays to M_s residuals calculated from the magnitude data in Table IV. (The rays which pass close to the North Pole were stopped close to that point due to ray-tracing numerical problems near

---

Geller, R. J. (1976). Scaling relations for earthquake source parameters and magnitude, Bull. Seism. Soc. Am., 66, 1501.

von Seggern, D., and R. Blandford (1972). Source time functions and spectra for underground nuclear explosions, Geophys. J., 31, 83.

von Seggern, D., and P. Sobel (1975). Experiments in refining M_s estimates for seismic events, SDAC Report No. TR-75-14, Teledyne Geotech, Alexandria, Virginia.

presumed to be an explosion on the basis of data to be presented later. The t* value for an f^{-2} source model is $-.01 \pm .19$ for the path to NORSAR and for an f^{-3} source model the t* value for the path to NORSAR is $-.20 \pm .18$. Since the value of t* cannot be less than zero, the t* value for the path to NORSAR is assumed to be zero for both the f^{-2} and f^{-3} source models. We add that there is a predominance of theoretical models which imply a f^{-3} source spectrum rather than an f^{-2} one (Geller, 1976). There appears to be a real difference in attenuation between the two paths. The Baikal to NORSAR paths have less attenuation than to LASA, as expected since the former path is mostly through continental shield areas while the latter path includes the anomalous upper mantle of the western United States. Values of t* for the Kazakh explosions for an f^{-2} source model (von Seggern and Blandford, 1972) were also calculated. These t* values are $.16 \pm .10$ for the East Kazakh to LASA path, $.05 \pm .08$ for the East Kazakh to NORSAR path, and $.23 \pm .10$ for the MILROW to LASA path. As expected from the reason just stated, the t* values for the paths to NORSAR are lower than the values for the paths to LASA.

von Seggern and Sobel (1975) have presented a method of predicting 20-second Rayleigh-wave amplitudes by geometrical ray tracing. Their work shows that lateral changes in 20-second LR phase velocity can cause major multipathing and also large teleseismic amplitude variations due to accumulated small-scale refraction effects. Figures 14 and 15 illustrate the paths of rays which result for events in the eastern and western parts of the rift zone. No attempt is made to quantitatively relate these patterns to observed LR amplitudes since we cannot correct the predicted amplitudes for source mechanism, but we can qualitatively compare the pattern of rays to M_s residuals calculated from the magnitude data in Table IV. (The rays which pass close to the North Pole were stopped close to that point due to ray-tracing numerical problems near

---

Geller, R. J. (1976). Scaling relations for earthquake source parameters and magnitude, Bull. Seism. Soc. Am., 66, 1501.

von Seggern, D., and R. Blandford (1972). Source time functions and spectra for underground nuclear explosions, Geophys. J., 31, 83.

von Seggern, D., and P. Sobel (1975). Experiments in refining M_s estimates for seismic events, SDAC Report No. TR-75-14, Teledyne Geotech, Alexandria, Virginia.

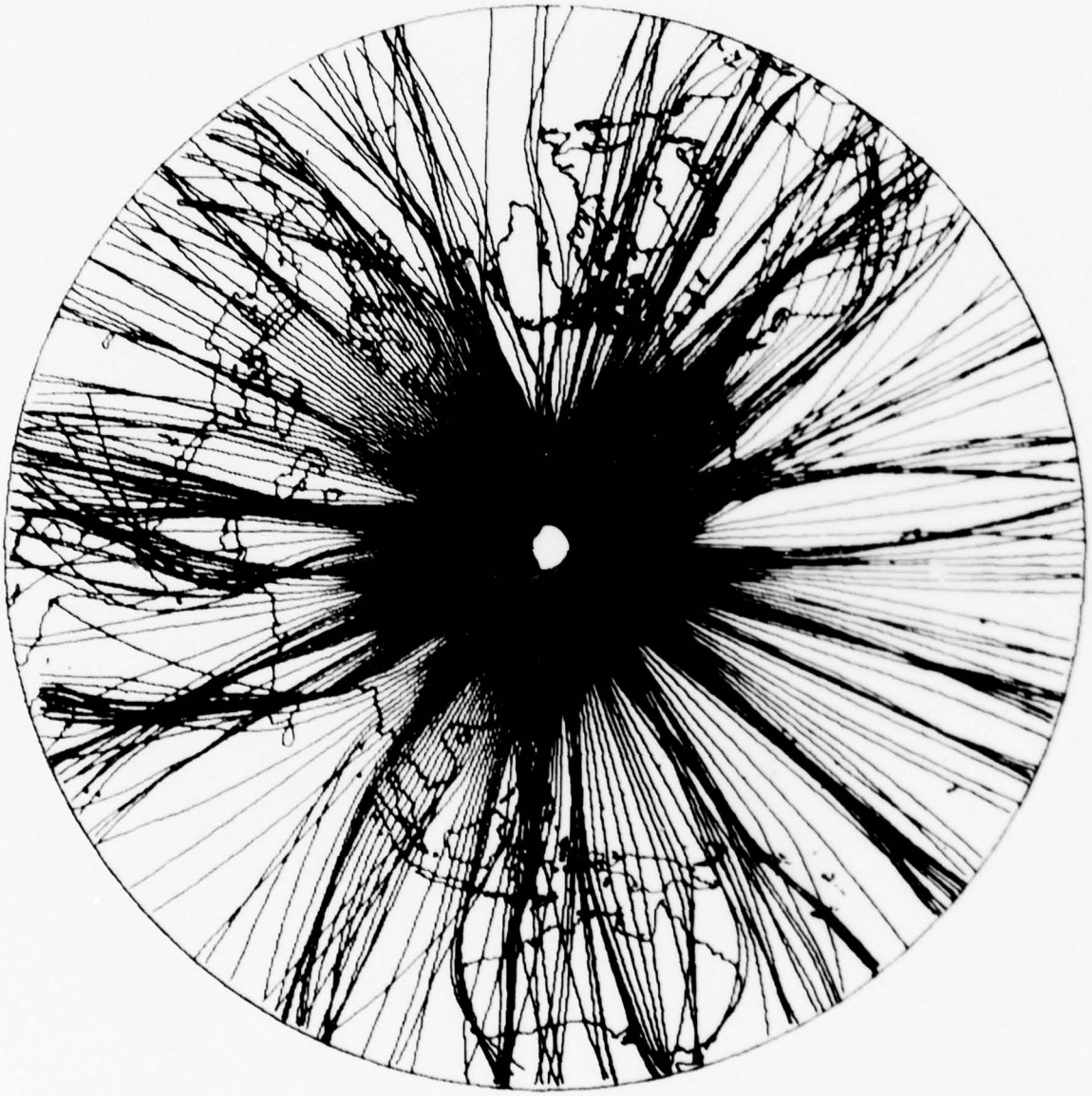

Figure 14. Predicted LR raypaths (T = 20 sec) for East Baikal (56.2N, 123.6E).

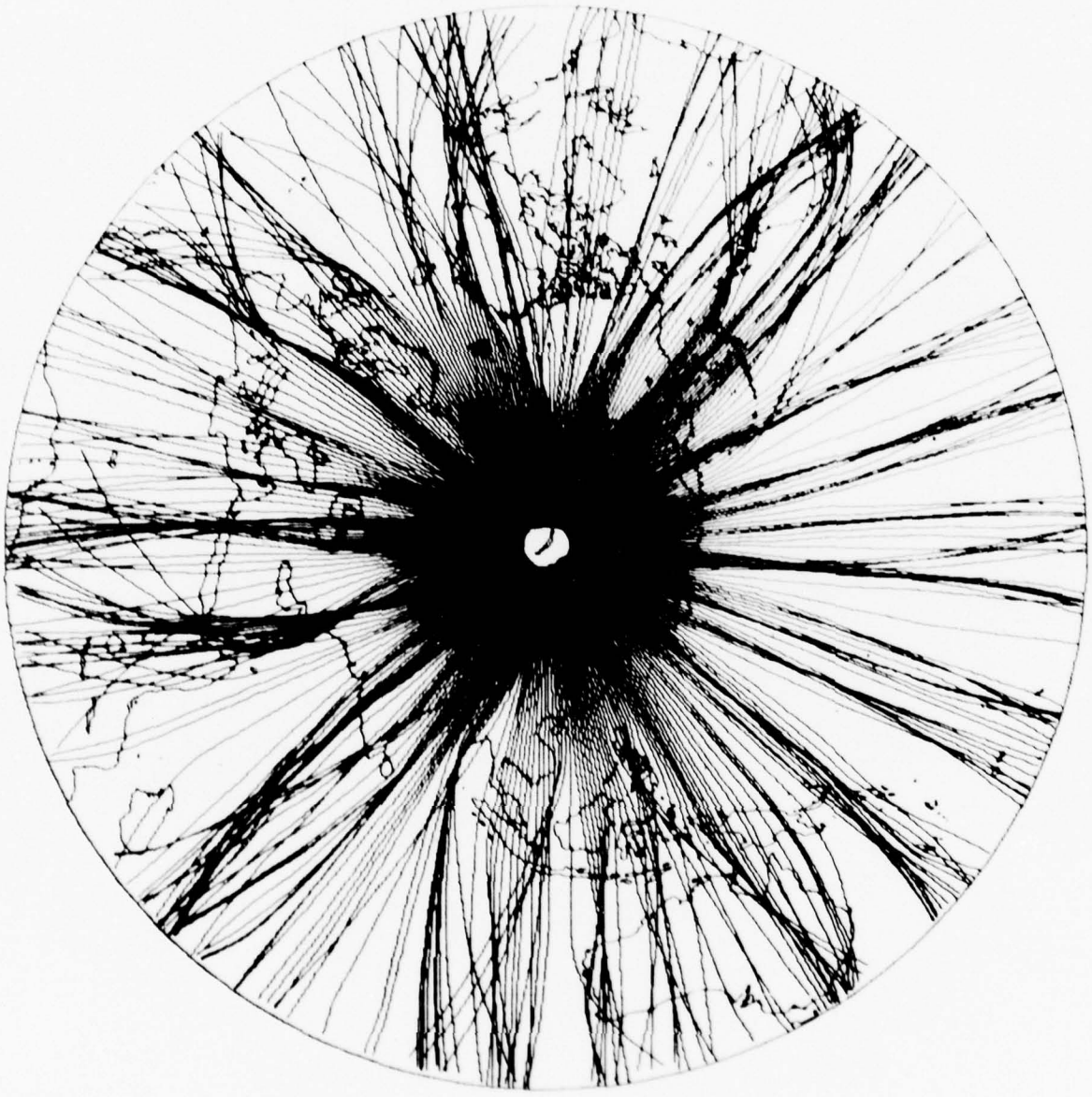

Figure 15. Predicted LR raypaths (T = 20 sec) for West Baikal (53.0N, 107.5E).

the poles.) Where the rays cross we can expect either constructive interference (large positive residuals as at NIL, OGD, and TOL/TLO) or destructive interference (large negative residuals as at JER and LASA). The M_s residuals at TAB in Iran are negative, as can be predicted from the diverging raypaths near that site. The M_s residuals at KON and NORSAR are positive as can be predicted from the converging ray paths near those sites, and the M_s residuals at QUE are about zero as can be predicted from the smooth ray pattern near that station. These results are only rough approximations since the velocity grid was not well known in some places and attenuation has not been taken into account. Also there are many recorded amplitudes which do not correlate well with the ray-tracing predictions. Stations which record a stable amplitude are desirable for calibrating a source region for amplitude. For events from the Baikal region, such stations could be located in Eastern Europe, Western USSR, and Eastern China. The complicated LR ray-tracing figures partially explain why we were unable to determine LR radiation patterns from our amplitude observations.

DISCRIMINATION ASPECTS

M_s-m_b

In this and the following sections we apply several common discriminants between earthquakes and explosions to the Baikal events, East Kazakh explosions, and MILROW. We independently determined average M_s and m_b values for the Baikal events in Table II using WWSSN stations, HGLP stations, the ALPA, LASA, and NORSAR arrays, and SRO data. The data used in the average estimates is listed in Table IV. Negative values in the table indicate noise measurements which were used as upper bounds for the signal amplitudes. Magnitudes were computed according to the formulas

$$m_b = \log (A/T) + B(\Delta)$$

$$M_s = \log (A/T) + 1.66 \log\Delta + 0.3$$

where A = one-half the peak-to-peak maximum recorded amplitude reduced to mμ ground displacements,

T = period in seconds (restricted to 17 to 23 sec for M_s calculations),

Δ = epicentral distance in degrees,

B(Δ) = Gutenberg-Richter correction term for surface-focus P waves.

We also independently determined M_s for the East Kazakh explosions in Table III using the NORSAR array and HGLP stations. The data used in the average estimates for explosion M_s are listed in Table V, and explosion m_b values are from the NEIS list. Note that the station distances for both the earthquakes and explosions (Table IV and V) are all teleseismic, and therefore regionalized magnitude formulas are not necessary. Throughout we have used a method of magnitude averaging proposed by Ringdal (1976) in which the magnitudes at the individual stations are assumed to follow a Guassian distribution. Among this distribution, amplitudes corresponding to some magnitudes will fall below the noise level. Ringdal's method then substitutes a noise measurement at those stations which don't detect and computes the maximum likelihood estimate of magnitude based on measured signals and noise estimates. The effect of this procedure is to more accurately define the magnitude of events not widely recorded. The M_s-m_b plot using this method for all the events of this study is shown in Figure 16.

Ringdal, F. (1976). Maximum-likelihood estimate of event magnitude, Bull. Seism. Soc. Am., 66, 789.

TABLE V

Magnitude Data for East Kazakh Explosions

Event 1

Station	Δ	M_s
CHG	35.1	3.23
AVERAGE		3.23

Event 2

Station	Δ	M_s
CHG	35.2	-3.47
EIL	38.1	-4.45
KON	38.9	3.59
NAO	38.0	3.49
AVERAGE		3.47

Event 3

Station	Δ	M_s
CHG	35.2	3.48
EIL	38.1	3.71
KON	38.9	3.59
NAO	38.9	3.96
AVERAGE		3.68

Event 4

Station	Δ	M_s
KON	39.1	-3.73
AVERAGE		-3.73

Event 5

Station	Δ	M_s
NAO	38.1	-2.69
OGD	85.9	
AVERAGE		-2.69

Event 6

Station	Δ	M_s
MAIO	41.5	
NAO	37.9	-3.1*
OGD	85.8	
AVERAGE		-3.1

*Bungum and Tjostheim, 1976

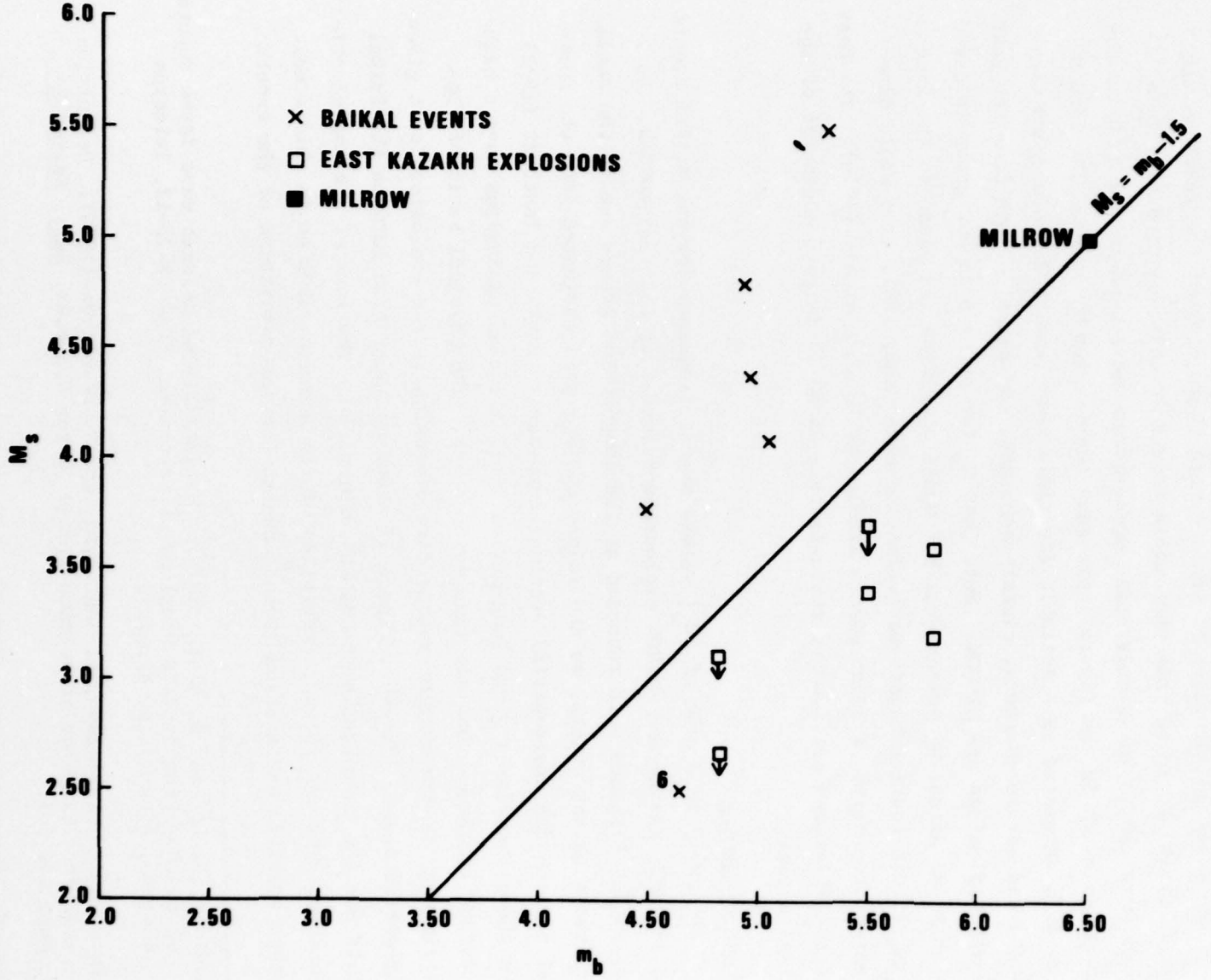

Figure 16. M_s vs. m_b for Baikal events and East Kazakh and MILROW explosions.

The magnitude averages of those events where many of the readings are noise levels are lower than what would result if only measured signal amplitudes were used. Where only noise measurements were used in the M_s determination, an arrow in the figure represents the maximum M_s value. The line $M_s = m_b - 1.5$, suggested as a suitable discrimination line by Blandford and Clark (1975) and earlier workers, clearly separates the Baikal events from the East Kazakh explosions and MILROW. Note that M_s for event 6 in our group is based on only one actual M_s measurement and would otherwise lie close to the line $M_s = m_b - 1.5$ if routine magnitude estimation were used. This line would also separate the suite of Asian events studied by Dahlman et al. (1974). The East Kazakh explosions are located approximately 15 to 30 degrees southwest of the Baikal events.

Corner Frequency

Figure 17 is a plot of $|\Omega_o|$ versus corner frequency for the Baikal events and the East Kazakh and MILROW explosions recorded at LASA and NORSAR. No long-period P phases were recorded at the long-period arrays due to the small magnitudes of the events, so the values of $|\Omega_o|$ were estimated from the spectral data of the short-period vertical component. Hanks and Thatcher (1972) have shown that for a given long-period level Aleutian explosions have a higher corner frequency than Aleutian earthquakes. The physical basis of this discriminant is the smaller source-time dimension of the explosion for a given long-period level. However, Figure 17 shows no separation between the Baikal events and the East Kazakh and MILROW explosions. The lack of a clear discriminant could be due to characteristics of the sources examined in this study. Another possible explanation is that due to the low magnitudes of the events

---

Blandford, R. R., and D. Clark (1975). Variability of seismic wave forms recorded at LASA from small subregions of Kamchatka, SDAC-TR-75-12, Teledyne Geotech, Alexandria, Virginia.

Dahlman, O., H. Israelson, A. Austegard, and G. Hornstrom (1974). Definition and identification of seismic events in the U.S.S.R., Bull. Seism. Soc. Am., 64, 607.

Hanks, T., and W. Thatcher (1972). A graphical representation of seismic source parameters, J. Geophys. Res., 77, 4393.

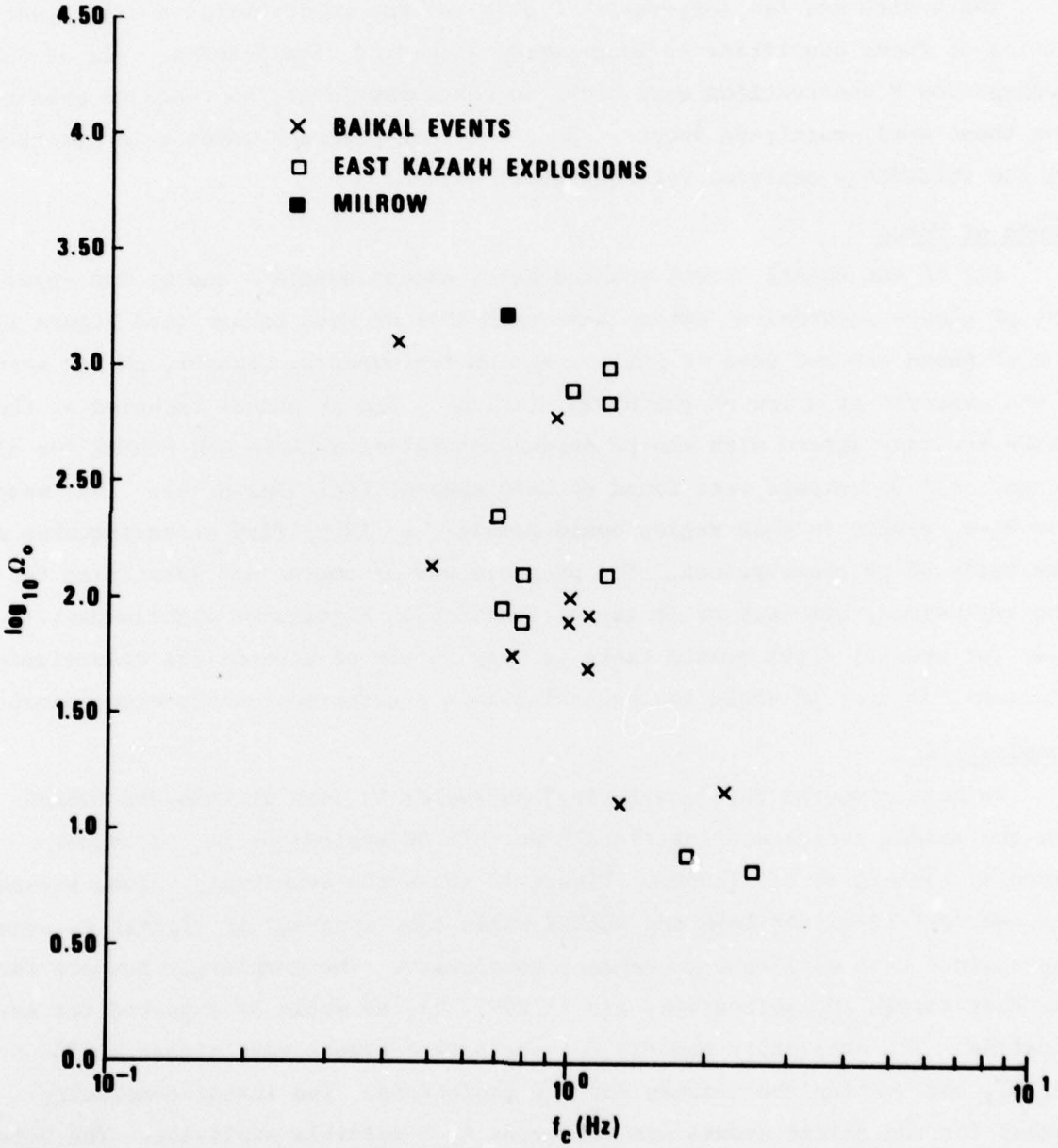

Figure 17. Long-period spectral level vs. corner frequency for Baikal events and East Kazakh and MILROW explosions from LASA and NORSAR P recordings.

studied here, a clear asymptotic value of $|\Omega_o|$ was not possible in most cases.

Long-Period Body-Wave Excitation

There were too few long-period P observations to determine average event ratios of these quantities to long-period LR ground displacement. All of the long-period P observations were close to the noise level, as would be expected for these small-magnitude events. No clear long-period S waves were observed on the recordings analyzed for the Baikal events.

Depth of Focus

All of the Baikal events studied here, except events 4 and 6, had apparent pP phases recorded at either LASA or NORSAR or both arrays (see Figure 2). The pP phase was not seen at LASA or NORSAR for event 4; however, pP for event 4 was observed at a few of the WWSSN stations. The pP phases recorded at the WWSSN stations agreed with the pP depths determined at LASA and NORSAR for all cases. All the events were found to have crustal foci (Table II). Thus many low M_s-m_b events in this region could possibly be identified as earthquakes on the basis of pP observations. The pP phase was of course not identified for the explosions, but lack of it cannot function as a positive discriminant. Also for crustal depth events there is very little pP moveout for teleseismic stations, so that pP would not be useful as a counter-shot-array discriminant.

Complexities

We have computed the "complexity" parameter as seen at LASA and NORSAR for the Baikal events and East Kazakh and MILROW explosions in the manner given by Lambert et al. (1969). Figure 18 shows the complexity values versus m_b. We reiterate that LASA and NORSAR beams show apparent pP signals in some cases since this will tend to enhance complexity. The complexity numbers for the East Kazakh explosions were low (3.27-7.35), as would be expected for explosions. The complexity numbers for the Baikal events were higher (4.14-13.36), but overlap the numbers for the explosions. The lowest complexity number for the Baikal events was for event 6, a possible explosion. The Baikal events with the exception of event 6 separate from the East Kazakh explo-

---

Lambert, D., D. von Seggern, S. Alexander, and G. Galat (1969). The LONGSHOT Experiment, Volume II. Comprehensive Analysis, SDL Report No. 234, Teledyne Geotech, Alexandria, Virginia.

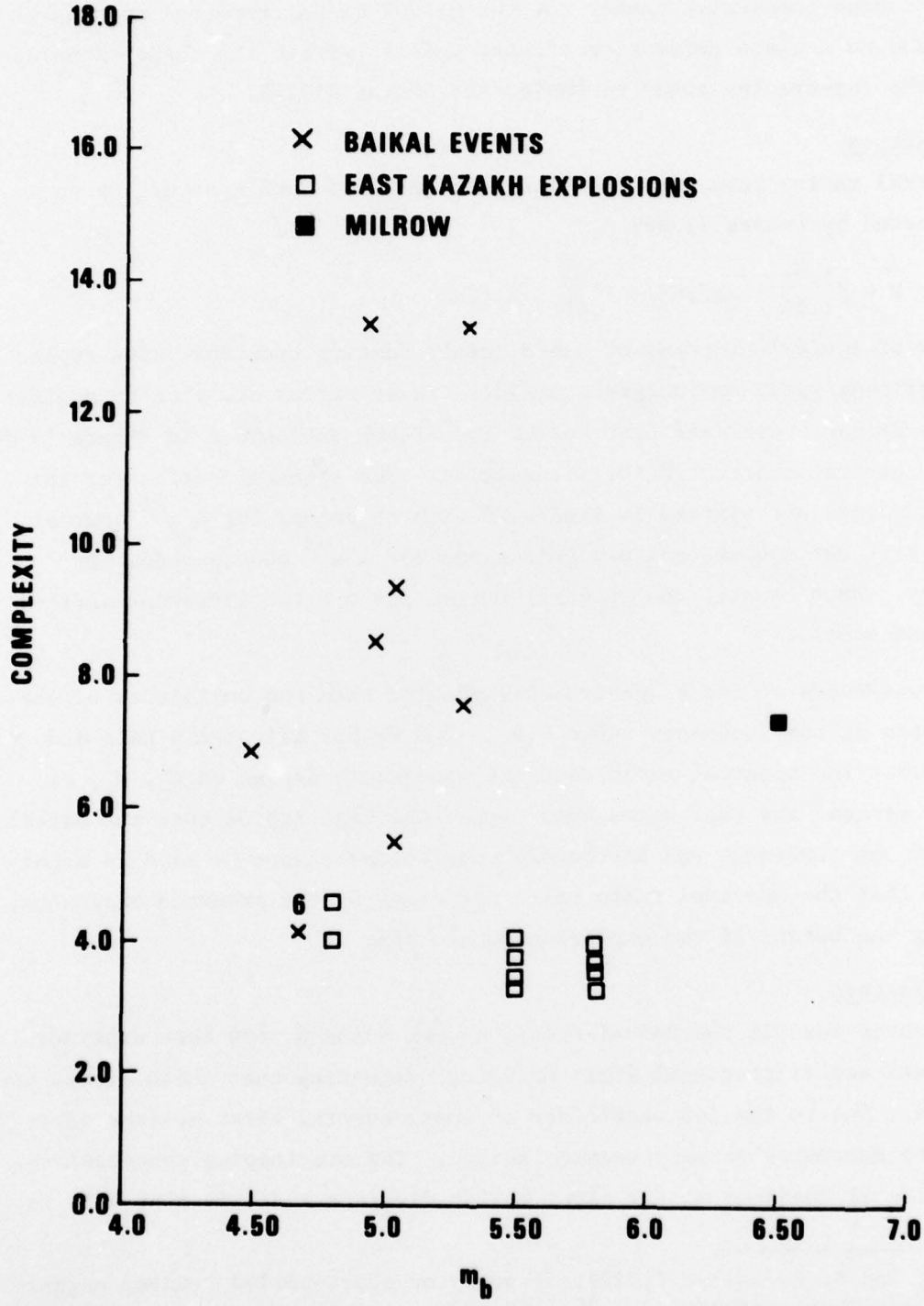

Figure 18. Complexity vs. m_b for Baikal events and East Kazakh and MILROW explosions from LASA and NORSAR P recordings.

sions. The high complexity number for the MILROW signal recorded at LASA is possibly due to a plate refraction effect; LASA is within the shadow zone defined by the ray-tracing study of Davies and Julian (1972).

Spectral Ratios

Spectral ratios have been calculated at LASA and NORSAR according to a form suggested by Lacoss (1969)

$$R = \int_{1.55}^{1.95} A(f)df \Big/ \int_{.45}^{.85} A(f)df$$

where sums of equivalent terms of the discrete Fourier transform have replaced the amplitude spectrum integrals A(f)df. These ratios are plotted against m_b for the Baikal events and East Kazakh and MILROW explosions in Figure 19 for using the spectra uncorrected for attenuation. The spectral ratios for the same P recordings are plotted in Figure 20 with t* values for a ω^{-2} source model for both earthquakes and explosions and for a ω^{-3} source model for earthquakes. Bars connect the spectral ratios for the two different earthquake source models.

The amplitudes of the P spectra were greater than the amplitudes of the noise spectra in the frequency range 0.4 to 2.0 Hz for all of the LASA and NORSAR beams. The spectral ratio does not apparently depend on m_b, M_s, or depth. In general the explosions show larger spectral ratios than the Baikal events, but the explosion and earthquake populations cannot be said to separate. Note that the spectral ratio value for event 6, the presumed explosion, falls along the border of the explosion population.

Radiation Pattern

Body waves for all the Baikal events except event 6 show both distinct compressional and dilatational first motions, suggesting that these events are earthquakes. Due to the low magnitudes of these events, first motions were difficult to determine on many records though. The overlapping compressional and dilatational readings on the first motion diagrams indicate that this is

---

Davies, D., and B. R. Julian (1972). A study of short-period P-waves signals from Long Shot, Geophys. J., 29, 195-202.

Lacoss, R. (1969). A large population LASA discrimination experiment, Technical Note 1969-24, Lincoln Laboratory, Lexington, Massachusetts.

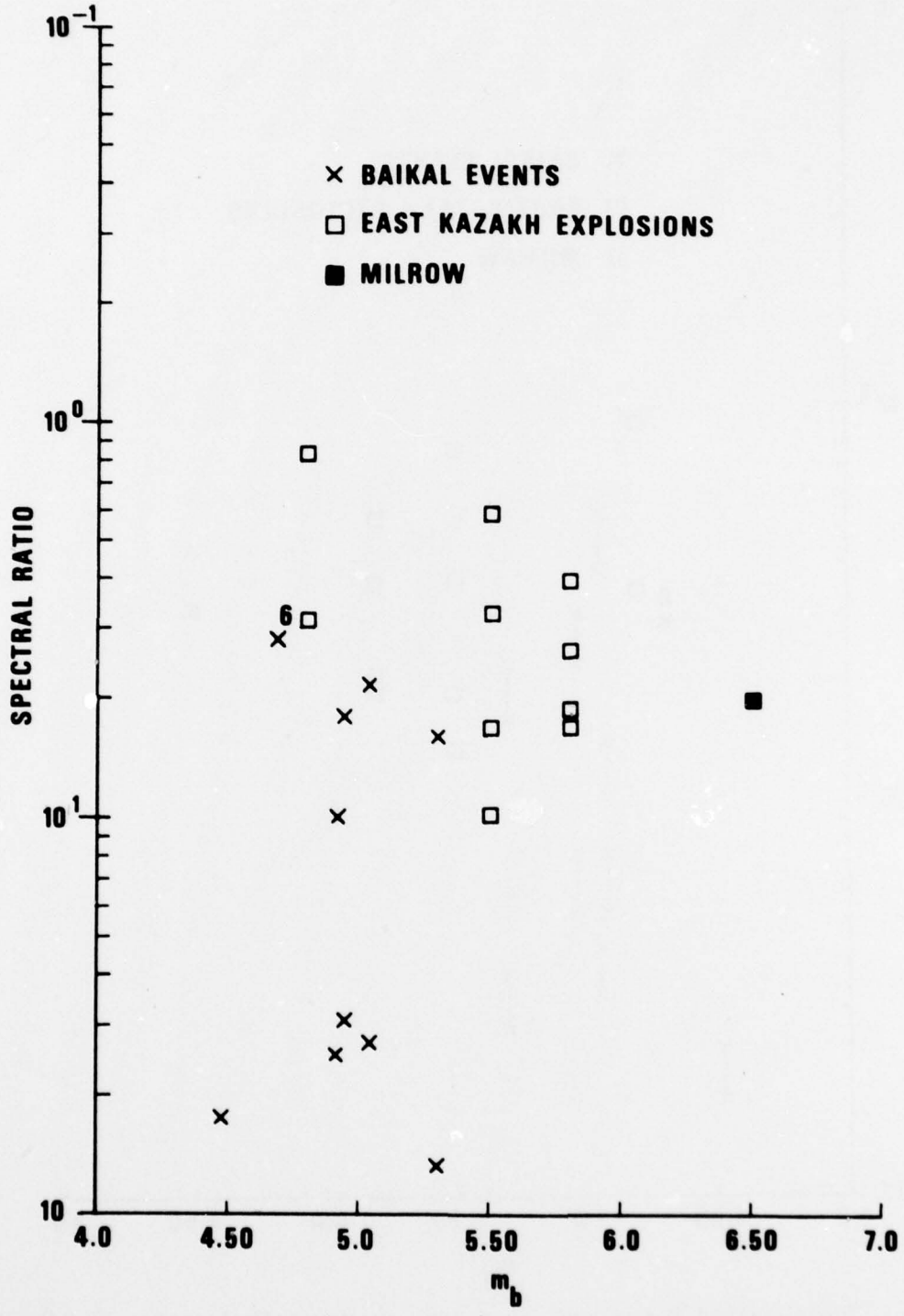

Figure 19. Short-period P spectral ratio vs. m_b for Baikal events and East Kazakh and MILROW explosions recorded at LASA and NORSAR for t* = 0.

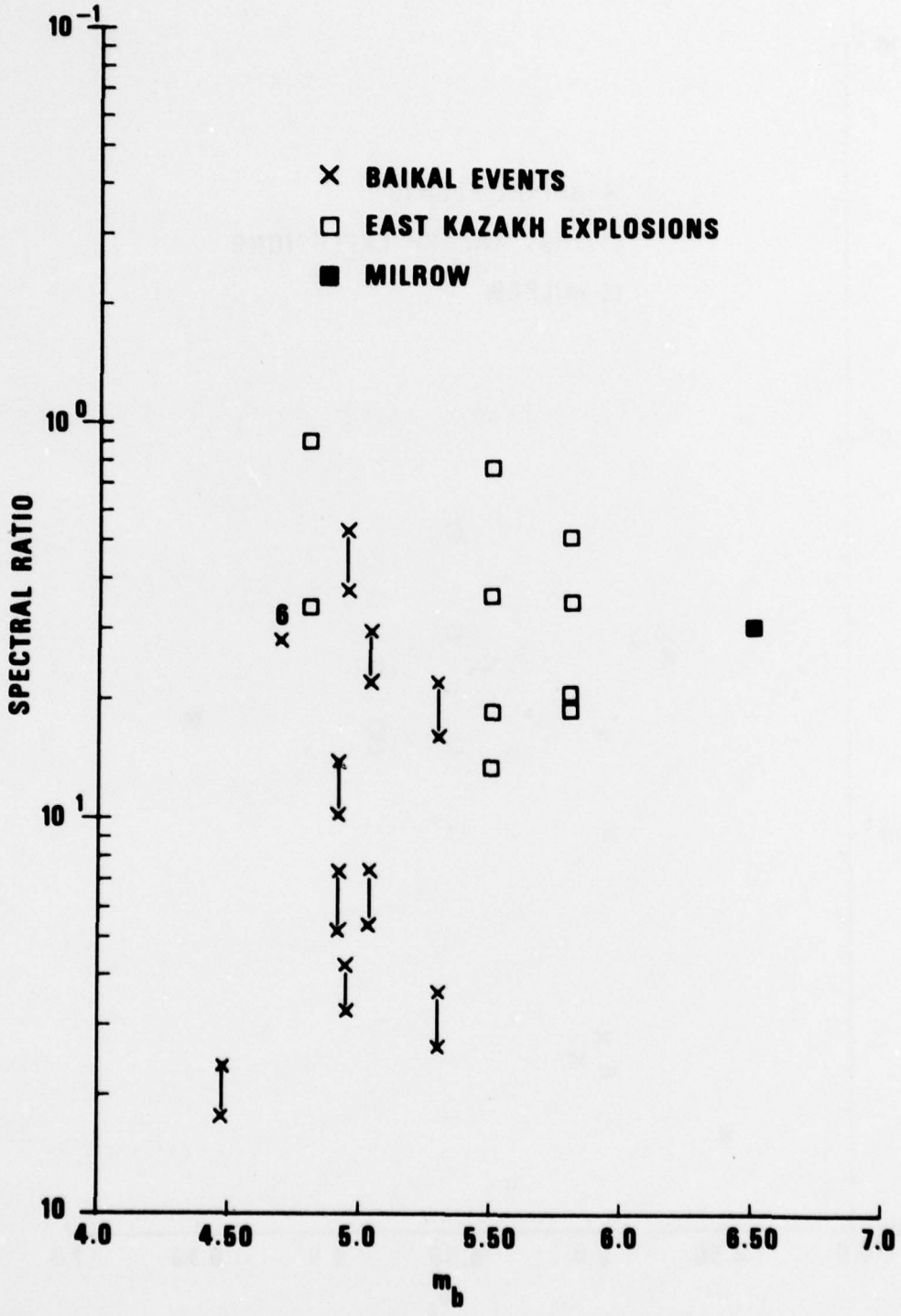

Figure 20. Short-period P spectral ratio vs. m_b for Baikal events and East Kazakh and MILROW explosions recorded at LASA and NORSAR. The t* values are for ω^{-2} source models for earthquakes and explosions and ω^{-3} source models for earthquakes.

not a reliable discriminant. We were not able to determine a radiation pattern from the LR amplitudes owing to the large scatter, which is caused by proagation effects, such as Q differences, dispersion effects on time-domain amplitudes, and focussing or defocussing due to refraction as illustrated in the predicted raypaths in Figures 14 and 15.

Short-Period Excitation

As might be expected for these small magnitude events, there were no short-period S observations from the Baikal events to determine the ratio of S/P ground displacement.

SUMMARY

Six events from the Baikal rift zone, six East Kazakh explosions, and the Aleutian explosion MILROW were examined in a seismic discrimination context. Most of the Baikal events lie close to major faults observed in satellite photographs. It was impossible on the basis of first motions to determine individual fault-plane solutions due to the small magnitudes of the events, but normal faulting may be indicated by the composite pattern. We were also unable to determine a radiation pattern from the LR amplitudes, probably due to widely varying propagation effects. The following characteristics of the Baikal events indicate that all the events except event 6 are earthquakes:

-- All the earthquakes (except #6) had apparent pP phases recroded at either LASA, NORSAR, and some the the WWSSN stations. Although little moveout can be detected for shallow earthquakes, identification of this phase is probably one of the best discriminants.

-- All the Baikal events studied here fall above the line $M_s = m_b - 1.5$, except event 6. The explosions clearly lie below the line $M_s = m_b - 1.5$.

-- Complexity separated Kazakh explosions from Baikal earthquakes in this data set, but only marginally so.

There are other areas in Asia, notably near 30°N, 95°E (Tatham et al., 1976), where earthquakes do not clearly separate from explosions in Asia on an M_s-m_b plot. Also shot arrays could be used to raise the M_s of an explosion by about 0.3 M_s units or more, placing it close to the earthquake population studied here.

We have concluded that event 6 was an explosion for the following reasons:

-- It was located north of the Baikal rift zone in an area where there are no active faults. (This "discriminant" would presumably not be available in case of a test ban treaty.)

-- There were no epicenters from 1971 through 1975 on the NEIS list within a few degrees of event 6.

Tatham, R. H., D. W. Forsyth, and L. R. Sykes (1976). The occurrence of anomalous seismic events in eastern Tibet, Geophys. J., v. 45, 451-481.

-- The long-period spectral level for event 6 falls within the explosion population.

-- There are no apparent pP phases recorded for event 6.

-- The complexity value for event 6 falls within the Kazakh explosion population. All the other Baikal events were separated from the Kazakh explosion population.

-- The spectral ratio for event 6 falls within the explosion population.

-- The M_s for event 6 is determined, on the basis of noise measurements and one observation, to be sufficiently low to characterize it as an explosion.

-- An origin time near the exact hour hints at a planned explosion.

In Figure 21 we present SRO recordings of P waves from this event. In each case, there seems to be a dilatational first motion. This contradicts our conclusion for the character of this source, and we suggest that these seismograms are blatant examples of the unreliability of first motion as a means of discriminating earthquakes from explosions. The noise in each case **might** distort the first motion considerably, such that the underlying compressional first break is obscured.

The low magnitudes of the earthquakes studied here (m_b from 4.48 to 5.30 and M_s from 3.56 to 5.49) made clear discrimination difficult with the available data and probably represent nearly the lowest threshold of multi-discriminant analysis for the stations used in this report. The installation of high quality SRO stations in Asia will permit the examination of lower magnitude events with multistation short-period data.

This study revealed little, if any, evidence for a highly attenuating upper mantle zone beneath the Baikal rift. A minor scan of ISC data resulted in no indication of a generally positive travel-time residual at stations near the zone, in fact the contrary. The values of t* computed from Baikal events to NORSAR and LASA were not significantly larger than for previous regions studied in this series of reports. The anomalous zone, if it exists, must be of limited extent, perhaps to be outlined by future detailed studies.

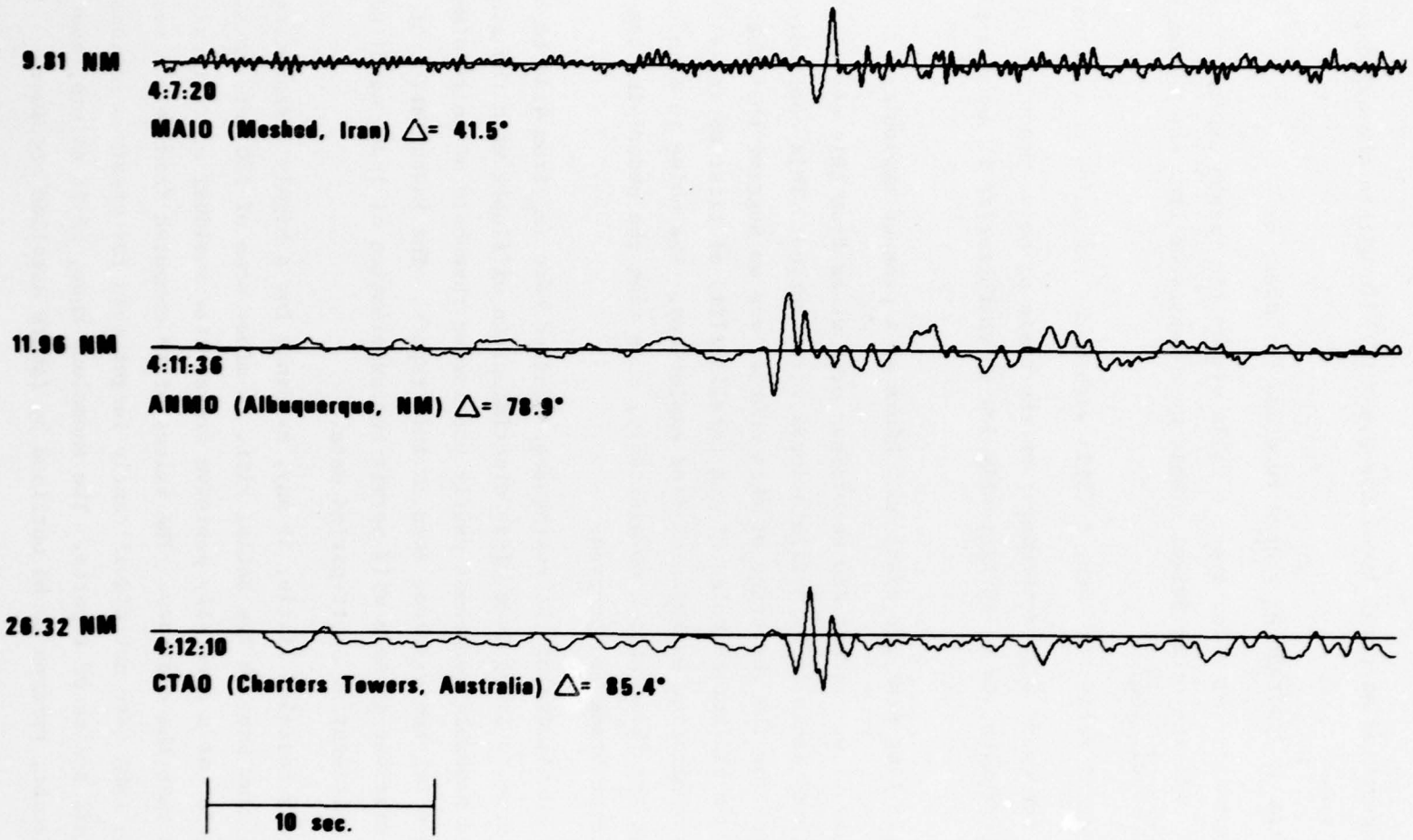

Figure 21. P-waves recorded at SRO stations for the 05 November 1976 Baikal event.

REFERENCES

Beliayevsky, N., A. Borisov, I. Valvovsky, and Y. Schukin (1968). Transcontinental crustal sections of the U.S.S.R. and adjacent areas, Canadian Journal of Earth Sciences, 5, 1067.

Ben-Menahem, A., S. Smith, and T. Teng (1965). A procedure for source studies from spectrums of long-period seismic body waves, Bull. Seism. Soc. Am., 55, 203.

Bradford, R. R. and D. Clark (1975). Variability of seismic wave forms recorded at LASA from small subregions of Kamchatka, SDAC-TR-75-12, Teledyne Geotech, Alexandria, Virginia.

Bungum, H., and D. Tjostheim, (1976). Discrimination between Eurasian earthquakes and underground explosions using the m_b:M_s method and short-period autoregressive parameters, Geophys. J., 45, 371.

Dahlman, O., H. Israelson, A. Austegard, and G. Hornstrom (1974). Definition and identification of seismic events in the U.S.S.R., Bull. Seism. Soc. Am., 64, 607.

Davies, D., and B. R. Julian (1972). A study of short-period P-waves signals from Long Shot, Geophys, J., 29, 195-202.

Der, Z. A. (1973). M_s-m_b characteristics of earthquakes in the East Himalayan regions. SDL report #296. Teledyne Geotech, Alexandria, Virginia.

Der, Z. A. (1976). On the existence, magnitude and causes of broad regional variations in body-wave amplitudes SDAC-TR-76-8, Teledyne Geotech, Alexandria, Virginia.

Geller, R. J. (1976). Scaling relations for earthquake source parameters and magnitude, Bull. Seism. Soc. Am., 66, 1501.

Hanks, T. and W. Thatcher (1972). A graphical representation of seismic source parameters, J. Geophys. Res., 77, 4393.

Lacoss, R. (1969). A large population LASA discrimination experiment, Technical Note 1969-24, Lincoln Laboratory, Lexington, Massachusetts.

Lambert, D., D. von Seggern, S. Alexander, and G. Galat (1969). The LONGSHOT Experiment, Volume II. Comprehensive Analysis, SDL Report No. 234, Teledyne Geotech, Alexandria, Virginia.

Lubimova, E. (1969). Heat flow patterns in Baikal and other rift zones, Tectonophysics, 8, 457.

Molnar, P., T. Fitch, and F. Wu (1973). Fault plane solutions of shallow earthquakes and contemporary tectonics in Asia, Earth and Planetary Science Letters, 19, 101.

Molnar, P., and P. Tapponier (1975). Cenozoic tectonics of Asia: effects of a continental collision, Science, 189, 419.

Puzyrev, N., M. Mandelbaum, S. Krylov, B. Mishenkin, G. Krupskaya, and G. Petrick (1973). Deep seismic investigations in the Baikal rift zone, Tectonophysics, 20, 85.

Ringdal. F. (1976). Maximum-likelihood estimate of event magnitude, Bull. Seism. Soc. Am., 66, 789.

Rodean, H. (1976). Seismic yield verification and a regional M_S versus m_b anomaly, Lawrence Livermore Laboratory, UCID-17006, 16 pp.

Solonenko, V. P. (1968). Regional seismic zoning of the U.S.S.R. - Eastern Siberia, in Seismic Zoning of the U.S.S.R., edited by S. V. Medvedev, English translation, Keter Publishing House, Jerusalem.

Tatham, R. H., D. W. Forsyth, and L. R. Sykes (1976). The occurrence of anomalous seismic events in eastern Tibet, Geophys. J., v. 45, 451, 481.

Vinnik, L., and A. Godzikovskaya (1972). Sounding of the Earth's mantle by the method of seismically conjugate points, Izvestia, Earth Physics, No. 10, 656.

Vinnik, L., and A. Godzikovskaya (1973). Lateral variations of the absorption by the upper mantle beneath Asia, Izvestia, Earth Physics, No. 1, 1.

von Seggern, D., and R. Blandford (1972). Source time functions and spectra for underground nuclear explosions, Geophys. J., 31, 83.

von Seggern, D., and P. Sobel (1975). Experiments in refining M_S estimates for seismic events, SDAC Report No. TR-75-17, Teledyne Geotech, Alexandria, Virginia.

Vvedenskaya, A. (1961). Special features of the stressed state in foci of earthquakes in the Baikal region, Izvestia, Geophys. Serv., 432.

Zorin, Y. (1971). Recent Structure and Isostasy of the Baikal Rift Zone and Surrounding Territory, Nauka, Moscow.